C.P. No. 890

MINISTRY OF AVIATION

AERONAUTICAL RESEARCH COUNCIL

CURRENT PAPERS

The Use of Air Injection to prevent Separation of the Turbulent Boundary Layer in Supersonic Flow

By

D. J. Peake, M.Sc.

LONDON HER MAJESTY'S STATIONERY OFFICE

1966

Price 12s 6d net

U.D.C. No. 532.526.3:533.6.011.5

C.P. No. 890

The use of air injection to prevent separation of the turbulent boundary layer in supersonic flow

- by -

D. J. Peake, M.Sc.

SUMMARY

An experiment has shown that a wall jet is able to prevent the separation of a turbulent boundary layer in a supersonic flow having a large pressure rise. The experiment was conducted with a mainstream Mach number of 1·8 upstream of the pressure rise at a Reynolds number of 4 million per foot.

A practical application of the work could be to supersonic air intakes. The potential performance of such an intake with injection boundary layer control appears to be about the same as that of an intake using suction control, but some of the design problems might be easier.

CONTENTS

TABLE

APPENDICES

ILLUSTRATIONS

ILLUSTRATIONS (cont'd)

1.0 Introduction

To obtain a satisfactory aerodynamic performance from a duct or wing, it is often necessary to apply a measure of control to the boundary layer flows. Methods are well known for preventing separation and controlling boundary layers on aerofoils in subsonic flow: the re-energisation of a boundary layer by blowing and control by suction are two common examples. A lack of fundamental information exists, however, on the effects of supersonic blowing in transonic and supersonic flow, where an additional complexity is that of shock/boundary layer interaction.

The control of a supersonic turbulent boundary layer can be important in practical applications. For instance, in a supersonic air intake the boundary layers in the supersonic and transonic regions are subjected to steep adverse pressure gradients generated by the intake shock system: if there were no boundary layer control, the flow would separate and thereby reduce the efficiency of diffusion. The favoured method of control, mainly because of its simplicity, is that of bleeding away the low energy air before or at incipient separation. Nevertheless, trouble is sometimes experienced in positioning and designing the bleed slots and in ducting away the low energy air; in addition, a loss of intake mass flow is incurred, often with a significant loss of performance associated with the bleed flow itself.

As an alternative to suction for the boundary layer control in an intake, supersonic air injection has been suggested, for it might overcome some of the difficulties associated with suction. The present investigation was planned, therefore, to produce data and an understanding of the flow fundamentals for supersonic blowing.

1.1 Previous work

In a theoretical analysis of blowing over flaps to achieve high lift on aerofoils[1] it has been proposed that, ideally, instantaneous mixing between the jet and the boundary layer would permit a pressure rise to be applied immediately without separating the boundary layer. For this ideal conception, it was reckoned that the excess momentum of the injection fluid should equal the momentum deficiency of the original boundary layer. It was pointed out, however, that in a practical flow the mixing of the two streams required a finite distance, and that a new wall boundary layer would grow under the jet. It was therefore suggested that about 2·5 times the ideal quantity of jet excess momentum might be necessary for a large pressure rise to be possible.

The results of some tests at transonic speeds performed at the National Physical Laboratory[2] showed that air injection reduced the effects of shock induced separation of the turbulent boundary layer. The injection of small quantities of air produced a large effect on the separation with the blowing slot in the dead air region. With the slot upstream of the separation, larger quantities of air were required to bring about an appreciable effect on the flow development. Lamson and Smetana[3] also found that blowing in the separation region yielded favourable results.

In subsonic flow and in a zero pressure gradient, Bradshaw and Gee[4] found that the jet excess momentum should be about 5 times the momentum deficiency of the original boundary layer for the velocity of the air in the original boundary layer to be eventually as great as the mainstream

value. In a positive pressure gradient, a value of jet excess momentum of about twice that of the original boundary layer momentum deficiency appeared adequate to prevent separation, but not enough to completely entrain the original boundary layer. It was thought that a method of calculation was unlikely to be found for a wall jet below a retarded stream until the generation of turbulent shear stress was understood fully.

An attempt was made by N.G.T.E. to re-energise by supersonic air injection the boundary layer on the sidewall of an intake where the flow direction had been reversed by shock wave/boundary layer interactions. A length of mixing of about 2 to 3·5 original boundary layer thicknesses was found to be insufficient. The inference was that blowing only slightly upstream of regions of separated flow did not necessarily produce the expected favourable effects - contrary to the results quoted in References 2 and 3; the conclusion reached was that a fundamental comprehension of the injection phenomena was necessary before re-energisation techniques could be justified in intakes.

Previous work has indicated, therefore, some confirmation and some contradiction between theoretical expectations and experimental results. It was hoped that the present investigation would produce evidence to help resolve the anomalies.

2.0 Apparatus

2.1 The wind tunnel

The rig is illustrated in Figures 1 to 3. The tunnel was supplied with dry air at a total pressure of 1 atm. abs. and was driven by a mechanical exhauster. The tunnel nozzle expanded the flow to a nominal Mach number of 1·9, which reduced subsequently to about 1·8 at the traverse region in the working section, downstream of the nozzle exit. The test boundary layer was that on the lower wall of the wind tunnel downstream of the nozzle throat, having an absolute thickness of about 0·25 in. at the traverse region. Throughout the tests, no provision was made for removing any boundary layers from those surfaces not associated with the test boundary layer. The rig aspect ratio of 2·53 when compared with previous work (References 5 to 9) appeared adequate to prevent any serious alteration of the test boundary layer on the centre-line by sidewall secondary flow. A discussion of such effects is given in Section 3.8.

A shock generator, or flap, was used as a means of subjecting the test flow to an adverse pressure gradient. The flap was installed in the top wall of the tunnel and had a range of deflection from 0 to 12°.

The first build of the working section (Figure 2) did not contain any provision for blowing. This build, the plain working section, was used to compare the quantities θ and δ of the test boundary layer with those given by theory, and to establish a reference boundary layer thickness with neither adverse pressure gradient nor injected air. The subsequent builds of working section (Figure 3) were equipped with a two-dimensional convergent-divergent blowing nozzle spanning the tunnel. The nozzle assembly was included in the lower wall which consisted of wood and Tufnol blocks. A choice of blocks and movement of the nozzle assembly enabled the position of air injection to be varied.

2.2 The injection nozzle

The two-dimensional nozzle profile is illustrated in Figure 4. The aim in designing the injection nozzle was to obtain a jet flow as uniform and as parallel to the mainstream as possible. However, straight tapered surfaces were prescribed for the supersonic expansion region of the nozzle as an accurately profiled upper wall with an associated thin lip (to prevent wake disturbances downstream) would have posed problems of lip deflection. To ensure a good flow distribution in the jet there was a 4/1 expansion ratio between the supply pipe and the reservoir and a 23/1 contraction ratio between the reservoir and the injection throat. The radius of curvature at the throat equalled 3·5 times the throat height - a value which is greater than the minimum suggested for good operation[11,12].

A design injection total pressure of about 2·5 atm. abs. was selected as providing a ratio of injection to mainstream total pressure representative of the values which might be available in practical applications. The nozzle area ratio was chosen to render the design mean static pressure at the nozzle exit equal to the constant static pressure through the undisturbed test boundary layer just upstream of the injection point. The corresponding Mach number of the injection flow was 2·37.

The blowing nozzle was considered large enough to prevent irregularities in the jet flow due to fine dust accretion - troubles with dust and problems of lip deflection had been encountered in the work reported in Reference 4. No attempt was made to simulate the three-dimensional mixing of Reference 10.

2.3 Instrumentation

Static pressure orifices were positioned along the lower wall for all the builds at the positions indicated in Figures 2 and 3.

Pitot pressures in the working section were measured using a probe[13] of 0·75 mm external diameter (0·018 in. i.d.), having a swan-neck to enable the probe tip to reach the wall. Distance measurements from the wall were corrected by adding a probe displacement value of 0·15 times the external diameter of the probe tip[14]. This value was used independently of Reynolds number and velocity gradient, but an additional correction was applied near the wall below a value of y equal to twice the external diameter of the probe tip[14]. A circular pitot probe was chosen rather than the rectangular or flattened type, as its displacement effects follow a predictable pattern in the turbulent boundary layer[15].

The pressure and temperature were measured at the tunnel inlet and in the supply pipe to the injection nozzle. An orifice plate[16] situated upstream of the injection throat measured the weight flow.

A conventional Schlieren apparatus provided flow visualisation.

3.0 Test results

A summary of the test results is shown in a qualitative and schematic form in Figure 5. The flow of the wall jet mixing with the original boundary layer is seen to consist of two regimes, the new wall boundary layer below the jet peak, and the mixing region, or wake. The tests indicate that reversal of either flow regime can happen. If the

pressure rise occurs a large distance downstream of the injection point the jet can be retarded to such an extent that reverse flow and separation of the new wall boundary layer can be provoked as in Figure 5(b). Alternatively if the pressure rise occurs very close to the injection point the static pressure may be greater than the minimum total pressure in the wake, so that the wake flow will be reversed as in Figure 5(c).

Tests were carried out with blowing pressures ranging between 1 and 2·5 atm. abs., typical results being given in Figure 7 onwards.

In the conversion of pitot pressure to total pressure a constant static pressure equal to the wall static pressure has been assumed through the flow from the wall to the mainstream, as nominal measurements of static pressure indicated a variation of not more than about 10 per cent of the wall value in any one traverse. No corrections were made for the effect of turbulence on the pitot readings, nor for the interaction between the flow and the shock wave from the probe. (These simplifications are thought to explain why some of the indicated jet peak total pressures exceed the pressure in the supply line.) The jet momentum has been specified as the excess momentum at the jet exit, $\left[m_J \left(u_J - u_1\right)\right]_e$, in order to correspond with the momentum deficiency of a boundary layer. The definitions are virtually the same except for sign:

$$\text{momentum deficiency} = \rho u_1^2 \theta = \int \rho u \left(u_1 - u\right) dy = \int \left(u_1 - u\right) dm.$$

The effects of temperature variations on the calculated excess momentum are discussed in Appendix II.

3.1 The original boundary layer or reference profile

A typical traverse in the plain working section (Figure 2) is shown in Figure 6, taken at a station where an oblique shock of wedge angle 5° would interact with the test boundary layer. The experimental velocity distribution is seen to be reasonably close to the empirical one seventh power law curve. The quantities θ and δ for the experimental profile agreed well with those given by the expressions for θ and δ in Reference 17. The values of mainstream velocity, u_r (= 1558 ft/s), absolute boundary layer thickness, δ_r (= 0·255 in.), and wall static pressure, p_r (= 5·36 in. Hg. abs.), were used as reference quantities when making later results non-dimensional.

3.2 Wall static pressure distributions

Figure 7 shows the pressure distributions along the wall, with the test points omitted for clarity.

It may be seen that the peak pressure increased with increase of shock generator angle, β, the highest pressure obtained being about 3·5 times the pressure level of the reference flow. For air injection at x = 11 in. and in some other tests, however, the peak value of the wall static pressure increased with the raising of the blowing pressure, whilst

β was held about constant. Some thoughts about this phenomenon are expressed in Section 3.6.

In all tests with adverse pressure gradient the expansion fan from the trailing edge of the deflected flap caused a sharp fall in the wall static pressure immediately after the shock interaction. Nevertheless, the object of the tests was to control the boundary layer to pass through the pressure rise, so that conditions downstream of the pressure rise were considered less important.

The uneven pressure distribution seen in Figure 7 upstream of the main pressure rise resulted from small surface discontinuities due to shrinkage of the wooden blocks.

3.3 Shock/boundary layer interaction in the plain working section with no air injection

Test A_2 of Figures 7 and 16(a) showed that a flow deflection angle of about 8° was necessary before separation occurred. The static pressure ratio of 1·8 agreed with the values given both by Beastall and Eggink[18] and by Fage and Sargent[19]. It is appreciably greater than for the three-dimensional interaction of a glancing shock wave with a turbulent boundary layer[20], where the corresponding value is about 1·5.

3.4 Total pressure and velocity profiles for the jet/boundary layer combination

Figures 8 t· 10 show some of the total pressure and velocity profiles for injection at 2 atm. abs. total pressure, each figure representing one position of the injection slot. Figure 11 shows the profiles when there is no pressure rise. The corresponding wall static pressure distribution is given on each figure together with the traverse locations.

Figure 8 shows the profile characteristics when the length of the mixing region - between the slot and the peak of the applied pressure rise - was equal to 10 times the thickness of the reference boundary layer. The entire flow is retarded as it passes through the pressure rise, the jet peak velocity being significantly reduced. The velocity profile upstream of the peak of the pressure rise indicates that the slower moving air in the boundary layer near the wall was retarded to an extent almost to produce flow reversal and consequent separation - compare with Figure 5(b). However, the raising of the blowing pressure to 2·5 atm. abs. enabled the flow to successfully negotiate a pressure ratio of about 3, as shown in the static pressure distributions of Figure 7.

In Figure 9 the length of the mixing region has been reduced to 6 reference boundary layer thicknesses. The mixing region is now much more retarded than in Figure 8 but the boundary layer under the jet is much less retarded and is appreciably thinner. Blowing at a total pressure of 2·5 atm. abs. permitted the flow to negotiate a static pressure ratio of 3·55.

When the mixing length was reduced to 2 reference oundary layer thicknesses, as in Figure 10, it appeared from the traverse just downstream of the peak of the pressure rise that the flow in the wake had reversed - the total pressure in the wake being less than the static pressure at the wall. The Schlieren pictures, however, suggested that the

flow successfully passed through the shock system. Either, therefore, the wake flow was quickly re-established with a positive velocity by rapid mixing, or the static pressure was greater at the wall than in the wake.

Figure 11 shows typical flow profiles with no applied pressure gradient. A tendency toward a constant value of wake trough velocity, u_t, of 0·8 u_r was evident following the initial fast rate of mixing between the jet and original boundary layer.

3.5 Some characteristics of the flow; criteria for control

The bulk of the original boundary layer was not immediately re-energised and entrained into the jet - presumably because the jet velocity was not much greater than that of the mainstream. The initial control mechanism was that of the jet taking the place of the original low energy layers at the wall, the low energy flow then being incorporated in a mixing region above the jet peak. At the same time, a new boundary layer developed at the wall under the jet. The total pressures of the wake trough and jet peak are plotted in Figures 12, 13 and 14, for the long, medium and short mixing regions respectively. For comparison, corresponding results for flow with and without a pressure rise are included on each sheet. The tests showed that the initial rate of mixing was rapid between the original boundary layer and the jet, and was approximately independent of the injection total pressure. A distance downstream of the injection point of 5 reference boundary layer thicknesses was required before the wake trough total pressure reached a value of 0·5 of the tunnel entry total pressure. Thereafter, the increase in the minimum total pressure of the wake was less rapid; a tendency toward a constant value of around 0·64 of the inlet total pressure was observed in the present experiment at a distance of 14 boundary layer thicknesses downstream of the jet exit.

With the long mixing region, as in Figure 12, the applied back pressure rise was of insufficient magnitude to reverse the wake flow. In Figure 14, however, as previously discussed, the wall static pressure exceeds the wake total pressure and it is suggested that the mixing region is too short. If in fact the wake is reversed the original boundary layer would be removed from the beneficial influence of the jet and eddy motions in the reversed wake flow region would tend to cause large mixing losses. Moreover in a diffuser reversal of the wake could lead to a breakdown of the whole supersonic flow. It is suggested, therefore, that the first criterion for control is that the locus of the applied static pressure distribution should be in the area below the locus of the wake trough total pressure; the wake should then present no problems of flow reversal. (Nevertheless, under some circumstances such as, for example, in Test Q of the present experiment, it should be noted that highly beneficial results may still be achieved, apparently, when the total pressure in the wake is somewhat less than the local wall static pressure.)

An obvious feature of all the flows was the rapid decrease of jet peak total pressure downstream of the injection point. Thus the second criterion for control is that at the position of the pressure rise the jet should not have lost momentum to an extent that the new wall boundary layer is in danger of separating. Figure 8 for example shows that the long mixing region is rather greater than the optimum for the present conditions, as the wall boundary layer is close to separation.

Thus the results show that with an injection to mainstream pressure ratio of 2/1 and for a mainstream Mach number of 1·8, the optimum position for the injection slot appears to be at about 6 reference boundary layer thicknesses upstream of the shock interaction region, with a jet excess momentum about equal to the momentum deficiency of the original boundary layer.

Johannesen[21] reported that the development of jets issuing into quiescent air at M = 1·40 was found to depend on the strength of the internal shock waves in the jet nozzle exit, the jet spreading rapidly but unsteadily in the presence of strong shocks. With no disturbance the spreading was far more gradual. The point may therefore be raised whether the internal disturbance in the jet due to the straight taper nozzle affected the initial mixing rate between the jet and the original boundary layer. This question cannot be satisfactorily answered here because of lack of experimental evidence.

3.6 The flow patterns

In discussing the flow patterns of the present experiment it is helpful first of all to review the standard results for the flow without injection. Some of the well known patterns are shown in Figure 15.

The extent of the upstream and downstream influence is small for weak shocks as in Figure 15(b). For stronger shocks, a separation bubble forms and gives rise to a shock upstream of the incidence point as in Figure 15(c). The Schlieren picture of Figure 16(a), for flow without boundary layer control, shows this configuration with its typical bifurcated shock system adjacent to the boundary layer.

Figure 15(d) shows the phenomenon of Mach reflection[22] which occurs when the Mach number downstream of the incident shock is less than the detachment Mach number. The shock system forms a normal leg at the wall, meeting the incident and reflected shocks at a triple point. The total pressures are not equal downstream of the normal and of the reflected shock so that a vortex sheet emanates from the triple point. A bifurcated foot to the normal leg generally appears when there is separation.

An example of the type of flow pattern obtained in the present experiment is shown in Figure 16(b), which illustrates a jet/boundary layer flow having profile characteristics similar to those shown in Figure 8, and the same mixing distance of 10 reference boundary layer thicknesses (Test G on Table I). The shock generator deflection is 12° giving a static pressure ratio of 3 at a blowing pressure of 2·5 atm. abs. A Mach reflection is seen with the normal leg passing through the viscous flow to the wall. There is no separation. A small discontinuity in the wall promotes a local shock expansion system upstream of the normal leg. The pitot probe is situated downstream of the normal leg in the viscous flow. The fact that the shock forms a Mach reflection is thought to explain the phenomena noted earlier, that the wall pressure rise increased with increase in blowing pressure even when the shock generator angle remained fixed. As the injection total pressure was increased the general level of Mach number would increase in the jet/boundary layer combination. Consequently the normal leg of the shock system would be expected to increase in strength - because of the rise in its upstream Mach number. In practical applications, therefore, the possible formation of Mach reflections should be kept in mind, lest a strong normal leg should cause difficulty.

3.7 Control of a boundary layer through a normal shock

The control of a boundary layer through a normal shock should present no complications additional to those already discussed. The wall static pressure distribution measured in the presence of the normal leg of a Mach reflection (e.g., Test Q on Figure 7) displays that the peak value of the pressure rise, 3·3, is only 8 per cent less than that of a normal shock whose upstream Mach number is that of the test mainstream - about 1·8.

An experiment was conducted with air injection at x = 9 in. to produce a normal shock to span the working section in the region of the previous shock wave/boundary layer interaction. A flat plate was inserted in the tunnel between the centre-line and the top wall, producing choking in the resultant upper passage and thereby generating a normal shock. Unfortunately, movement of the pitot probe in the interaction region upset the stability of the shock configuration, so that traverses were not possible. It was noted, however, that when injecting air at 2 atm. abs. total pressure, a shock pressure ratio of 3·35 produced a small region of wall boundary layer separation. In retrospect, this result could have been predicted from the corresponding profile characteristics described in Section 3.4 and shown in Figure 8, where it was seen that for a shock pressure ratio of 2·8 the wall boundary layer was close to separation. A rather better result would have been expected from the use of the medium length mixing region.

3.8 Three-dimensional flow effects in nominally two-dimensional flow

Gadd and Holder[8] have commented that there are discrepancies between different experiments regarding the extent of the ineraction region when oblique shock waves interact with turbulent boundary layers. The discrepancies may be due to the entrainment into the test boundary layer of sidewall secondary flow, produced by the interaction between the oblique shocks and the sidewall boundary layers of the test rig. It is desirable, therefore, to have as large a span of test boundary layer as possible in order to avoid three-dimensional cross flow components of velocity.

The ratio of the span to the height of the working section, that is, the geometric aspect ratio, employed in the present work was 2·53. Bogdonoff and his fellow workers[5,6] used a test boundary layer on the wall of a wind tunnel of aspect ratio 1·25, whilst the rigs at the National Physical Laboratory[7,8] and the wind tunnel used by Seddon[9] all had aspect ratios less than unity. Perhaps a more appropriate comparison to use, rather than one based on the cross-section dimensions of the wind tunnel, would be that of the ratio of the span of the test boundary layer to either (a), the length of the test boundary layer, or (b), the length of the sidewall boundary layer - for the extent of interaction of a shock wave with a turbulent boundary layer is roughly proportional to the boundary layer thickness, which is in turn roughly proportional to the length of surface on which the test boundary layer is growing. A comparison shows that the ratios for (a) and (b) for the present work are of the same order as estimates made for the ratios of the rigs described in References 5, 6, 8 and 9. Furthermore, Kuehn, in Reference 23 and during later work of his discussed in Reference 8, found that where the sidewall boundary layers were about the same thickness as the test boundary layer (as in the present rig)

a closer approximation to two-dimensional results was obtained than with a test arrangement where the test boundary layer was much thinner than the sidewall boundary layers.

It appears, therefore, that the rig chosen for the present work should not have given appreciably worse three-dimensional flows than the rigs used by other workers, so that in this sense the flow in the present tests was nominally two-dimensional. Even so, it is felt that future work should preferably be conducted in rigs of higher geometric aspect ratio.

4.0 Analysis

4.1 Comparison of the velocity in the wake trough with that deduced by a semi-empirical method

In Reference 24 Spence investigated the velocity defect of turbulent wakes behind aerofoils in subsonic flow. He concluded that the locus of the minimum velocity in the wake followed a universal recovery law of the form:

$$\frac{u_t}{u_1} = 1 - \frac{K_1}{\left(\frac{x}{c} + k_1\right)^{\frac{1}{2}}} \qquad \ldots.(1)$$

where u_t was the wake trough velocity and c the aerofoil chord. Spence found that $K_1 = 0{\cdot}1265$ and $k_1 = 0{\cdot}025$ gave the best fit with experiment; also, a velocity ratio of 0·2 was obtained at the trailing edge because of a fairing in of the cusp in the velocity profile at that point. All the data came from tests in a Reynolds number range from 0·5 to 5 million.

In the present experiments a similar analysis can be attempted for the wake downstream of the injection slot. A plot was therefore made, Figure 17, of the wake trough velocity, u_t, against distance downstream of the injection point. In order to make u_t non-dimensional it was divided by an average of the local mainstream and jet/peak velocities, i.e., by $u_a = \left(\frac{u_1 + u_j}{2}\right)$; the velocities u_1 and u_j were those at the wake extremities. Non-dimensional lengths downstream of the injection point were also evolved by using a denominator $L_1 = \left(\frac{\ell_1 + \ell_2}{2}\right)$, based on the wetted surface lengths of the two boundary layers meeting at the trailing edge of the jet nozzle, namely the original boundary layer and the jet boundary layer on the upper wall of the jet nozzle. The length L_1 corresponded to the aerofoil chord, c, that Spence used. The growth of the boundary layer in each supersonic nozzle was taken to be the same as that on a flat plate of length equal to two thirds of the distance from the throat to the nozzle exit. The Reynolds number based on L_1 and u_a was about 2 million.

The results from all the experimental groups with air injection for flow with and without adverse pressure gradient are plotted in Figure 17. It is seen that a curve of the form:

$$\frac{u_t}{u_a} = 1 - \frac{K_2}{\left(\frac{x - x_e}{L_1} + k_2 \right)^{\frac{1}{2}}} \qquad \ldots.(2)$$

where $K_2 = 0{\cdot}10$ and $k_2 = 0{\cdot}025$, provides a reasonable description of the minimum velocity in the wake in the regions where the applied pressure rise is not large. When the wake flow is retarded severely by a sharp adverse pressure gradient the wake trough has velocity values well below the curve of Equation (2). The lowering of the constant in the numerator of Equation (2) when compared with Equation (1) follows from the usual result that the rate of mixing is less for compressible than for incompressible flow. A simple differentiation of Equation (1) or (2) indicates that the velocity gradient with respect to x is proportional to the constant in the numerator, so that the smaller the constant the smaller is the mixing rate.

4.2 The wall boundary layer under the jet peak

Schwarz and Cosart in Reference 25, summarising previous results as well as their own for incompressible turbulent wall jets, suggested that as a first order engineering approximation the inner layer of the wall jet could be considered analogous to the one seventh power law turbulent boundary layer. Nevertheless, certain dissimilarities were posed between the two types of flow.

A comparison between measured wall boundary layer thicknesses and theoretical growths calculated using the method given in Reference 17 was made for Tests F and K, that is, with air injection at $x_e = 9$ in. and a blowing pressure of 2 atm. abs. Stratford and Beavers[18] used the well known equation for absolute boundary layer thickness (although previously it had been used in a more restricted sense):

$$\delta = 0{\cdot}37 \, X \, R_X^{-\frac{1}{5}} \qquad \ldots.(3)$$

where the boundary layer growth over an equivalent distance X at constant Mach number M equalled the growth along the actual surface whose final mainstream Mach number was M. The superficial utilisation of:- (a) the full equations from Reference 17 (since the jet peak Mach number was decreasing downstream) and then, as an alternative, (b) placing X equal to the actual length of surface on which the wall boundary layer grew downstream of the injection throat, permitted a trial of two preliminary methods of assessment. Both methods were found to over-estimate the boundary layer thicknesses under the jet. In the region of zero and adverse pressure gradient the maximum discrepancy for (b) equalled 14 per cent of the measured value, while for (a) it was much higher. Also, downstream of the peak static pressure rise the theoretical estimate was totally inaccurate. Thus, the method of calculation of Reference 17 was not appropriate to the present flow, indicating that the properties of the

wall boundary layer under the jet were not the same as for an ordinary boundary layer under a mainstream. In Reference 17, the reduction of the mainstream Mach number is assumed to be caused entirely by the pressure rise, whereas in the present flow the reduction in the jet peak Mach number is partly due to mixing. In addition once the jet has become fully developed it has some resemblance to fully developed pipe flow - in which the thickness of the "boundary layer" remains constant.

4.3 Use of the momentum equation

The momentum equation for steady compressible flow may be expressed in the form:

$$(\partial/\partial x)(\rho_1 u_1^2\theta) = \tau_w + \delta^*\partial p/\partial x \qquad \ldots\ldots(4)$$

where the symbols have their usual meaning (see list in Appendix I). In order to find whether the momentum equation could be used for the theoretical prediction of the present type of flow the experimental results could be substituted into Equation (4). However, the differentiation of experimental values of $(\rho_1 u_1^2\theta)$ would probably lead to serious errors, so that an integrated form of Equation (4):

$$\frac{(\rho_1 u_1^2\theta)_x}{(\rho_1 u_1^2\theta)_o} = \frac{1}{(\rho_1 u_1^2\theta)_o}\left\{\left(\rho_1 u_1^2\theta\right)_e + \int_e^x \tau_w dx + \int_e^x \delta^* dp\right\} \qquad \ldots\ldots(5)$$

where suffix o denotes quantities of the original boundary layer, is more suitable as a test of the experimental results.

The simplest flow to examine first is that without pressure gradient, for which Equation (5) reduces to:

$$\frac{(\rho_1 u_1^2\theta)_x}{(\rho_1 u_1^2\theta)_o} = \frac{1}{(\rho_1 u_1^2\theta)_o}\left\{\left(\rho_1 u_1^2\theta\right)_e + \int_e^x \tau_w dx\right\} \qquad \ldots\ldots(6)$$

Values of θ for Test K were calculated from the traverse profiles by graphical integration while an expression for the wall shear stress in a zero pressure gradient was derived as in Appendix III. Figure 18 shows that these quantities are consistent with Equation (6) to a very satisfactory accuracy.

The corresponding analysis for the flow with pressure gradient is not easy, mainly because of the difficulty in finding a suitable expression for the wall shear stress. One test showed reasonable agreement with Equation (5) but the results are not quoted as the analysis for the wall stress was not felt to be fully satisfactory.

The results for the flow without a pressure rise show that the momentum equation is satisfied, and it seems probable that the equation could be used in general when predicting theoretically the mixing of a jet with a turbulent boundary layer.

4.4 Practical applications; the pressure recovery of a supersonic intake with injection boundary layer control

In Reference 2 the work on injection was aimed at improving the controls on an aircraft at transonic speeds. Another possible application is to the control of boundary layers in supersonic air intakes - especially in axisymmetric intakes having combined external/internal compression. The design of the centrebody in an axisymmetric intake incorporating some internal compression can make it difficult to lead out the boundary layer bleed. Injection boundary layer control - shown by the present work to be feasible in the large pressure rises obtaining in an intake - would pose fewer installation problems as a pressurised duct system to the injection slots would require less space than boundary layer bleed passages.

The present results may be used to predict the pressure recovery that would seem feasible in a supersonic air intake with injection boundary layer control. The static pressure rise obtained in the present investigation would be roughly the same as that obtained in an intake between the blowing slot and a position immediately downstream of the normal shock, provided the slot were located at a station where the mainstream Mach number equalled about 1·7 to 1·8. In Appendix IV, an expression for the mean total pressure that might be expected at the exit from the subsonic diffuser is derived as Equation (19).

On the basis of Equation (19a) a calculation for an axisymmetric intake[27] with external/internal compression at a mainstream Mach number of 3, and for full scale Reynolds number, gave a mean total pressure at the compressor face of 93 per cent for an injection mass flow equal to about 11 per cent of the capture flow. The injection mass flow is consistent with calculations in Reference 28, which showed that 13 per cent of the capture flow compressed to 2/1 pressure ratio would just overcome the momentum deficiencies of the intake boundary layers. An 'effective cost' of the injection in terms of pressure recovery was estimated in Reference 28 to be about 10 per cent, the cost being taken as the additional pressure drop required across the turbine in order to provide the power needed to compress the recirculating mass flow. These results indicate that the feasible overall performance of the intake chosen would be about the same as that given by theoretical estimates for suction boundary layer control. The final advantage between the two control techniques, therefore, could be dependent upon their respective practical convenience.

5.0 Conclusions

(1) Air injection can prevent a supersonic turbulent boundary layer separating in a large pressure rise. In the present tests control could be maintained up to static pressure ratios of 3, provided the jet excess momentum was about equal to the momentum deficiency of the original boundary layer. The optimum position for the injection slot appeared to be a distance upstream of the main part of the pressure rise equal to about six times the thickness of the initial boundary layer.

(2) Two criteria need to be satisfied in order to avoid flow reversal: (a) the total pressure in the wake from the original boundary layer must be greater than the local value of the static pressure - otherwise reversal of the wake flow will result; (b) the fall off in the jet peak total pressure must not be so severe that the new wall boundary layer is in danger of separating.

(3) When the pressure rise is small, the velocity defect in the wake from the original boundary layer is roughly proportional to the inverse square root of the distance downstream of the blowing slot.

(4) The flow quantities closely satisfy the momentum equation, at least for the flow without a pressure rise. Consequently the equation might be utilised in predicting the characteristics of a jet mixing with a boundary layer - perhaps in conjunction with the correlation of the velocity in the wake mentioned in conclusion (3).

(5) The test results may be used to deduce the pressure recovery which seems feasible in a supersonic air intake with injection boundary layer control.

ACKNOWLEDGEMENTS

The author would like to thank Dr. B. S. Stratford for the suggestion of the project and useful discussion throughout the course of the work and Mr. E. Hemmings for his invaluable co-operation with the building and modification of the rig; also to Dr. G. E. Gadd of the National Physical Laboratory for a discussion on three-dimensional effects and for drawing the author's attention to Reference 8.

REFERENCES

No.	Author(s)	Title, etc.
1	B. S. Stratford	Boundary layer control by injection from aircraft gas turbine engines. A.R.C. 16137 FM1949, July, 1953.
2	A. Chinneck Miss G. C. A. Jones Miss C. M. Tracey	Interim report on the use of blowing to reduce the fall in control effectiveness associated with shock induced separation at transonic speeds. A.R.C. 17564 FM2231, April, 1955.
3	P. Lamson F. Smetana	Investigation of circulation control. USCEC Rept. 49-101 (p.12, VI:Blowing in supersonic flow), March, 1958.
4	P. Bradshaw M. T. Gee	Turbulent wall jets with and without an external stream. A.R.C. R. & M. 3252, 1962.
5	S. M. Bogdonoff C. E. Kepler E. Sanlorenzo	A study of shock wave turbulent boundary layer interaction at M = 3. Princeton Univ. Aero Eng. Rept. 222, July, 1953.
6	I. E. Vas S. M. Bogdonoff	Interaction of a turbulent boundary layer with a step at M = 3.85. Princeton Univ. Aero. Eng. Rept. 295, April, 1955.
7	D. W. Holder H. H. Pearcey G. E. Gadd	The interaction between shock waves and boundary layers. A.R.C. 16077 FM1937, July, 1953.
8	G. E. Gadd D. W. Holder	The behaviour of supersonic boundary layers in the presence of shock waves. 7th Anglo-American Aeronautical Conference, New York, October, 1959. Institute of Aeronautical Science Paper (59-138), 1959.
9	J. Seddon	The flow produced by interaction of a turbulent boundary layer with a normal shock wave of strength sufficient to cause separation. A.R.C. 22637 FM3062, March, 1960.
10	R. A. Wallis	A preliminary note on a modified type of air jet for boundary layer control. A.R.C. 18440 FM2404, May, 1956.

REFERENCES (cont'd)

No.	Author(s)	Title, etc.
11	L. Howarth	Modern developments in fluid dynamics: High speed flow. Vol. II, p. 497 to 499 Oxford Univ. Press, 1953.
12	J. B. McGarry	The development of a variable Mach number effuser. A.R.C. R. & M. 3097, 1958.
13	J. C. Ascough	The development of a nozzle for absolute airflow measurement by pitot-static traverse. A.R.C. R. & M. 3384, 1964.
14	F. A. Macmillan	Experiments on pitot tubes in shear flow. A.R.C. R. & M. 3028, 1957.
15	S. Dhawan B. R. Vasudeva	The pitot tube displacement effect in boundary layer flows. Jour. Ae. Soc. India, February, 1959.
16	British Standards Institution	British Standard Code BS.1042, 1943 - Flow measurement.
17	B. S. Stratford G. S. Beavers	The calculation of the compressible turbulent boundary layer in an arbitrary pressure gradient - a correlation of certain previous methods. A.R.C. R. & M. 3207, 1961.
18	D. Beastall H. Eggink	Some experiments on breakaway in supersonic flow. Part I R.A.E. Tech. Note Aero. 2041 (1950) Part II R.A.E. Tech. Note Aero. 2061 (1950)
19	A. Fage R. Sargent	Shock wave and boundary layer phenomena near a flat plate surface. Proc. Roy. Soc. A, 190, 1 to 20, (1947)
20	A. Stanbrook	An experimental study of the glancing interaction between a shock wave and a turbulent boundary layer. A.R.C. C.P. 555, 1960.
21	N. H. Johannesen	The mixing of free axially symmetrical jets of Mach number 1.40. A.R.C. R. & M. 3292, 1959.
22	H. W. Liepman A. Roshko	Elements of gas dynamics, p. 106. Galcit Aero. Series, John Wiley & Sons, Inc. New York, March, 1958.

REFERENCE (cont'd)

No.	Author(s)	Title, etc.
23	D. M. Kuehn	Experimental investigation of the pressure rise required for the incipient separation of turbulent boundary layers in two-dimensional supersonic flow. N.A.S.A. Memorandum 1-21-59A, February, 1959.
24	D. A. Spence	Growth of the turbulent wake close behind an aerofoil at incidence. A.R.C. 14953 Tech. Rept. C.P. No. 125, 1953.
25	W. H. Schwarz W. P. Cosart	The two-dimensional turbulent wall jet. Jour. Fluid Mechanics, Vol. 10, Part 4 June, 1961.
26	L. Howarth	Modern developments in fluid dynamics: High speed flow. Vol. I, p. 456 to 462 Oxford Univ. Press 1953.
27	D. J. Peake	Unpublished M.O.A. Report.
28	P. G. Street	The design of axisymmetric centrebody intakes having internal compression. A.R.C. 23063 E.A.851, August, 1961.

TABLE I

Test configurations

Test	wedge angle β^0	Injection location $\frac{x}{L}$, x in.	Injection total pressure / Tunnel inlet total pressure $\frac{P_I}{P_{IN}}$	Remarks	
A: A_1	5			Plain working section: no blow	
A_2	8				
B	6	0.545, 9		No blow	
C	6	0.545, 9	1		With adverse pressure gradient
D	10.5	0.545, 9	1		
E	11.5	0.545, 9	1.5		
F	11.5	0.545, 9	2		
G	12	0.545, 9	2.5		
H	0	0.545, 9		No blow	No adverse pressure gradient
I	0	0.545, 9	1		
J	0	0.545, 9	1.5		
K	0	0.545, 9	2		
L	0	0.545, 9	2.5		
M	10	0.606,10	1		With adverse pressure gradient
N	10.5	0.606,10	2		
O: O_1	11	0.606,10	1.5	Wall static pressure only	
O_2	11	0.606,10	2.5		
P	10	0.666,11	1		With adverse pressure gradient
Q	10	0.666,11	2		
R: R_1	10	0.666,11	1.5	Wall static pressure only	
R_2	10	0.666,11	2.5		

APPENDIX I

~~List of~~ Symbols

x	distance downstream from the exit of the tunnel nozzle
X	an equivalent distance
y	distance normal to the wall
L	length of the working section
M	Mach number
u	velocity in x direction
ρ	density
m	mass flow
n	exponent in the power law relationship for a turbulent boundary layer
P	total pressure
p	wall static pressure
τ	shear stress
ν	kinematic viscosity
δ	absolute thickness of the boundary layer, or jet/boundary layer combination

$$\delta^* = \delta_r \int_0^{\delta/\delta_r} \left(1 - \frac{\rho u}{\rho_1 u_1}\right) d\left(\frac{y}{\delta_r}\right), \text{ displacement thickness}$$

$$\theta = \delta_r \int_0^{\delta/\delta_r} \frac{\rho u}{\rho_1 u_1}\left(1 - \frac{u}{u_1}\right) d\left(\frac{y}{\delta_r}\right), \text{ momentum thickness}$$

β — angle to the flow of the shock generator

K_1, K_2, k_1, k_2 — experimentally determined constants

α — area total pressure deficiency in two-dimensional flow, non-dimensional

$$= \int_0^{\delta} (P_1 - P)dy \Big/ \int_0^{\delta_0} (P_1 - P)dy_0$$

Suffices

o — original boundary layer upstream of the injection point

e — location of the injection nozzle exit

I — injection reservoir conditions

IN — tunnel mainstream reservoir conditions (upstream of tunnel nozzle)

J — jet peak

1 — local mainstream

r — reference profile, (undisturbed boundary layer with no air injection)

t — wake trough

w — wall

APPENDIX II

The effect of temperature

In many of the tests the jet total temperature was about 5 per cent greater than that of the mainstream, a difference which could significantly affect the value of $(u_j - u_1)$ in the calculation discussed in Section 3.0 for jet excess momentum. However, the apparent effect of temperature, using the criterion of jet excess momentum as here defined, is probably not a genuine one. For example, if a hot jet of fairly low total pressure mixed ideally with a boundary layer and produced a flow of uniform velocity equal to the mainstream velocity, the total pressure in the boundary layer/jet combination would still be low and hence there could be a rapid retardation and a reverse flow in a subsequent pressure rise. Consequently both total pressure and momentum must be considered. Now the performance of a conventional ejector of given geometry and fixed primary pressure ratio is virtually independent of changes in the primary temperature (other than for the fact that the primary mass flow required to choke the nozzle is proportional to $T^{-\frac{1}{2}}$). It would seem, therefore, that the criterion of excess momentum as here defined should be applied only to a flow with a uniform temperature: having, say, specified the total pressure of injection and the area of the injection nozzle such as to satisfy the criterion of excess momentum in a flow with uniform temperature, variations of temperature could be applied without significantly affecting performance, other than for the $T^{-\frac{1}{2}}$ factor on mass flow. By applying these arguments it has seemed justifiable in the analysis of the present experiment to ignore the small temperature variations.

APPENDIX III

The wall shear stress for a zero pressure gradient

The wall shear stress in compressible flow with zero pressure gradient may be written:

$$\tau_w = \frac{d}{dx}(\rho_1 u_1^2 \theta) = \rho_1 u_1^2 \frac{d\theta}{dx} \qquad \ldots\ldots(7)$$

Reference 18 quotes that for compressible flow the momentum thickness θ for a turbulent boundary layer on a flat plate in a semi-infinite mainstream is:

$$\theta = 0.036\, x R_x^{-\frac{1}{5}} \left(1 + \frac{M^2}{10}\right)^{-0.70} \qquad \ldots\ldots(8)$$

In the present work the jet peak values are the effective mainstream values for calculating the wall shear stress downstream of the injection nozzle.

$$\therefore \tau_w = 0.036\, \rho_J u_J^3 \left(1 + \frac{M_J^2}{10}\right)^{-0.70} \frac{d}{dx_J}\left[x_J \left(\frac{u_J x_J}{\nu_J}\right)^{-\frac{1}{5}}\right]$$

$$= 0.029\, \rho_J u_J^3 \left(1 + \frac{M_J^2}{10}\right)^{-0.70} \left(\frac{u_J x_J}{\nu_J}\right)^{-\frac{1}{5}} \qquad \ldots\ldots(9)$$

where $x_J = x - x_e + \ell_2$ and ℓ_2 is defined in Section 4.1.
Since the growth of the wall boundary layer in the experiment is less than that of a true turbulent boundary layer on a flat plate for corresponding values of x_j, the value of τ_w should strictly have been obtained in terms of δ_J and not in terms of x_J, in a similar way to the consideration of turbulent flow in a pipe. For an ordinary turbulent boundary layer, $\tau_w \propto x^{-\frac{1}{5}}$ and $\delta \propto x^{\frac{4}{5}}$, so that $\tau_w \propto \delta^{-\frac{1}{4}}$. Thus, strictly, the flat plate wall shear stress of Equation (9) should be factored by the ratio $\left(\frac{\delta \text{ flat plate}}{\delta \text{ actual}}\right)^{\frac{1}{4}}$ to give the actual value of wall shear stress. It may be seen that the effect of this ratio is small. A typical difference

between the respective values of δ is of the order of 20 per cent and would only produce an error of about 5 per cent in the estimation of τ_w. A further justification for using an expression for τ_w in terms of x_j is that a formula in terms of δ may only be used when δ is known. Thus, the formula in terms of x_j is a more practicable one provided it is reasonably accurate.

APPENDIX IV

Calculation of the pressure recovery of a supersonic intake having injection boundary layer control

The performance of an engine designed for supersonic flight depends to a large extent on the pressure recovery of the air intake and the losses associated with the boundary layer control. In an intake in which the boundary layer is controlled by air injection, the total pressure losses would be those due to friction and mixing along the walls of the duct and those related to the compression of the mainstream through the intake shock wave system.

Let the total pressure of the mainstream at the capture plane be P_C. At a station such as DD in Figure 19(a) just downstream of the throat normal shock, let the cross-sectional area be A_D (suffix D referring to the station DD) and the mean total pressure $\bar{P}_D$. Then:

$$\bar{P}_D = P_C - \frac{\text{losses due to friction and mixing}}{A_D} - \text{shock losses}$$

the shock losses being expressed in the conventional manner as a proportion of the total pressure, whereas the losses due to friction and mixing are assumed to be an integral of pressure over a cross-sectional area. Also "losses due to friction and mixing" is used as a general term to include all the effects of injection, being taken negative where the total pressure exceeds the local mainstream value.

If the losses due to friction and mixing at any station are together denoted F and the shock losses S, then

$$\bar{P}_D = P_C - F_D/A_D - S_D \qquad \ldots\ldots(10)$$

Let δ be the thickness of the jet/boundary layer combination, measured from the wall to the mainstream. If δ is small compared with the cross-sectional dimensions, the losses at DD due to friction and mixing may be referred to as an area total pressure deficiency and represented as:

$$\int_0^{\delta_D} (P_1 - P)\, dy_D$$

per unit distance around the perimeter, where P_1 is the total pressure in the local mainstream. If dZ_D is an increment of the wetted perimeter at DD, the area total pressure deficiency is:

$$F_D = \int_{Z_D} dZ_D \int_0^{\delta_D} (P_1 - P)\, dy_D \qquad \ldots\ldots(11)$$

Allowing a value for the total pressure loss in the subsonic diffuser of, say, 0.03 P_C, the total pressure recovery at the compressor face EE - Figure 19(a) - may be expressed as either:

$$\frac{\overline{P}_E}{P_C} = 1 - \alpha_D \frac{F_o}{A_D P_C} - \frac{S_D}{P_C} - 0.03 \qquad \ldots.(19a)$$

or

$$\frac{\overline{P}_E}{P_C} = 1 - \alpha_D \frac{A_o}{A_D} \left\{ 1 - \frac{\overline{P}_o}{P_C} - \frac{S_o}{P_C} \right\} - \frac{S_D}{P_C} - 0.03 \qquad \ldots.(19b)$$

Equation (19a), in conjunction with Equation (12), is probably the most convenient when working from a theoretical calculation of the growth of the original boundary layer - and Equation (19b) when from an experimental traverse.

FIG. 1

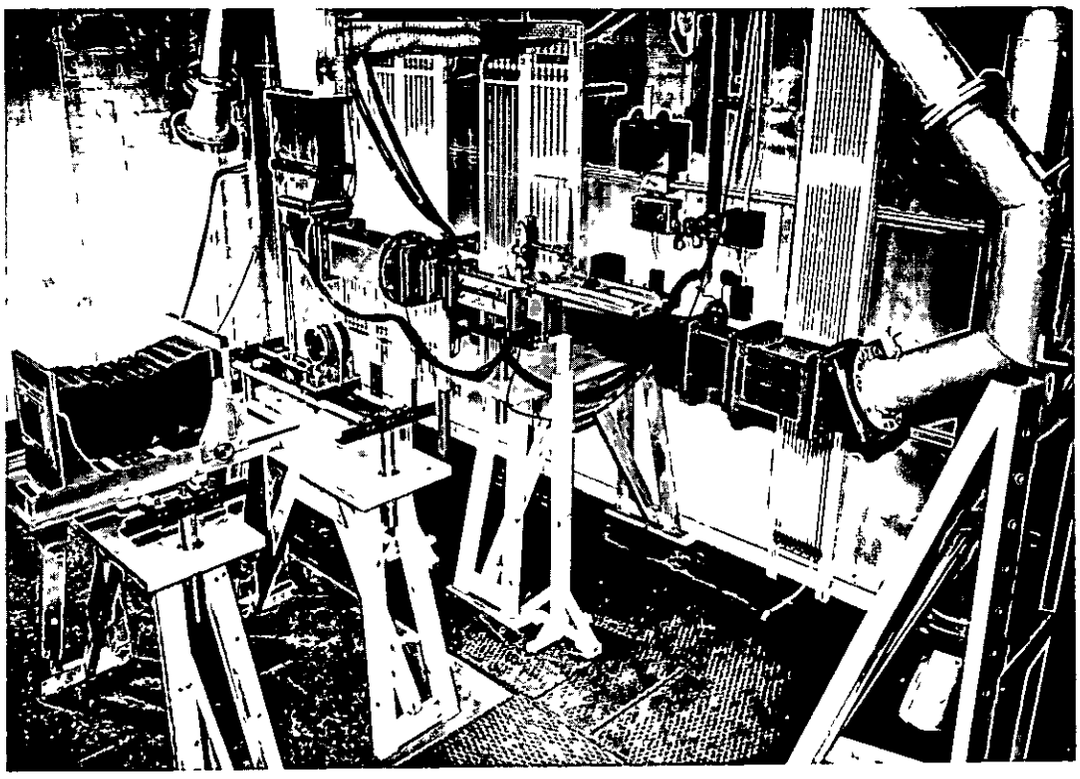

(a) GENERAL VIEW

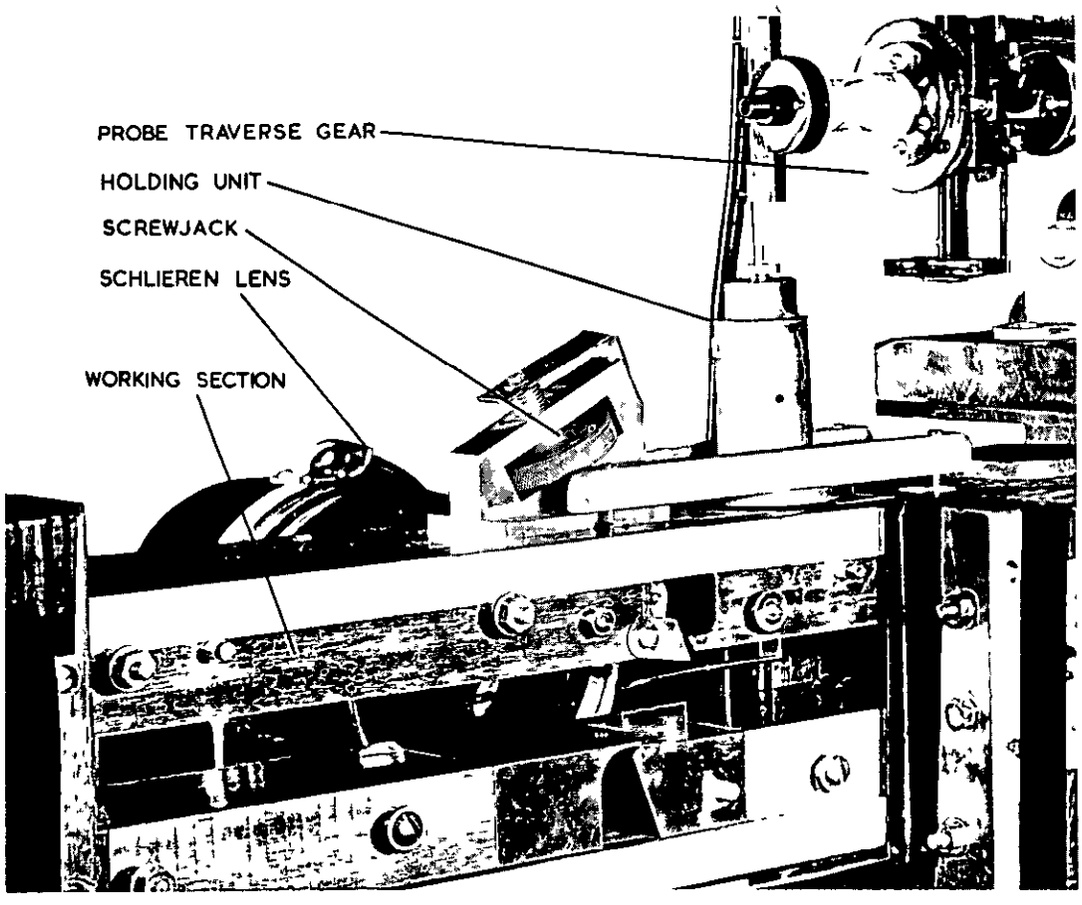

(b) THE WORKING SECTION WITH THE INJECTION NOZZLE ASSEMBLY

THE RIG.

FIG. 2

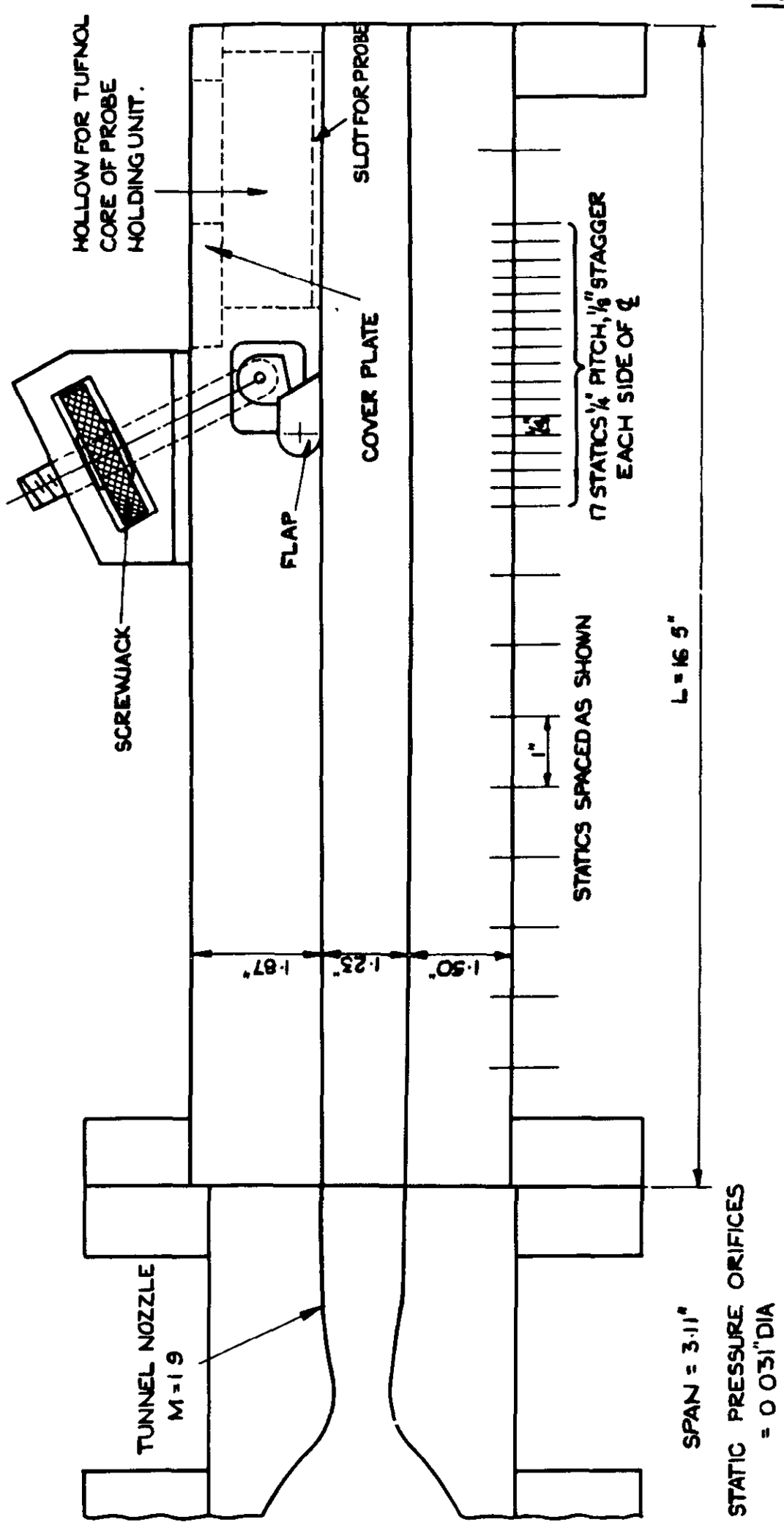

PLAIN WORKING SECTION
(WITHOUT BLOWING NOZZLE)

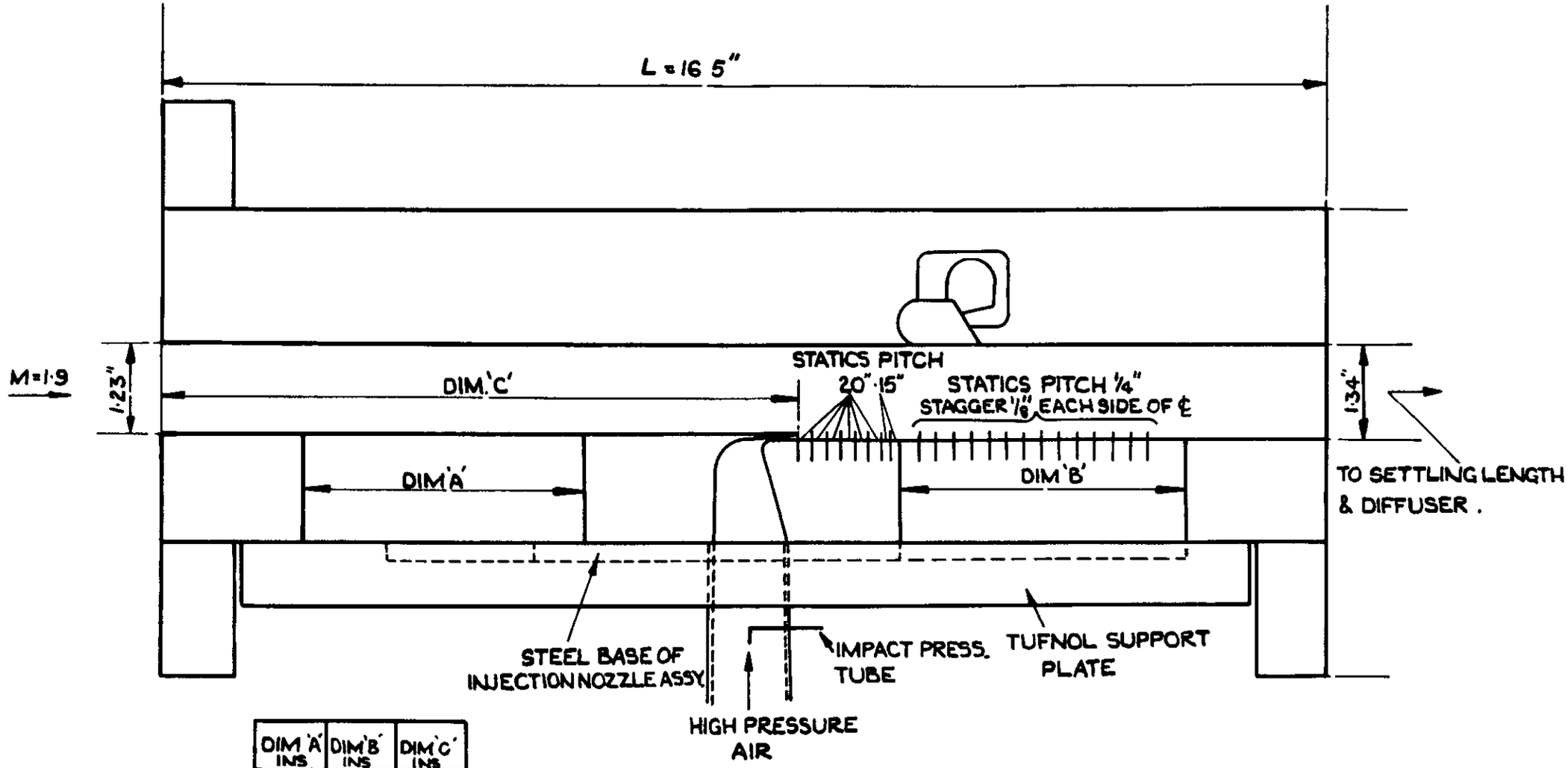

DIM 'A' INS	DIM 'B' INS	DIM 'C' INS
4·0	4·0	9·0
5·0	3·0	10·0
6·0	2·0	11 0

SPAN = 3·11"

WORKING SECTION WITH
BLOWING NOZZLE

FIG.3

FIG. 4

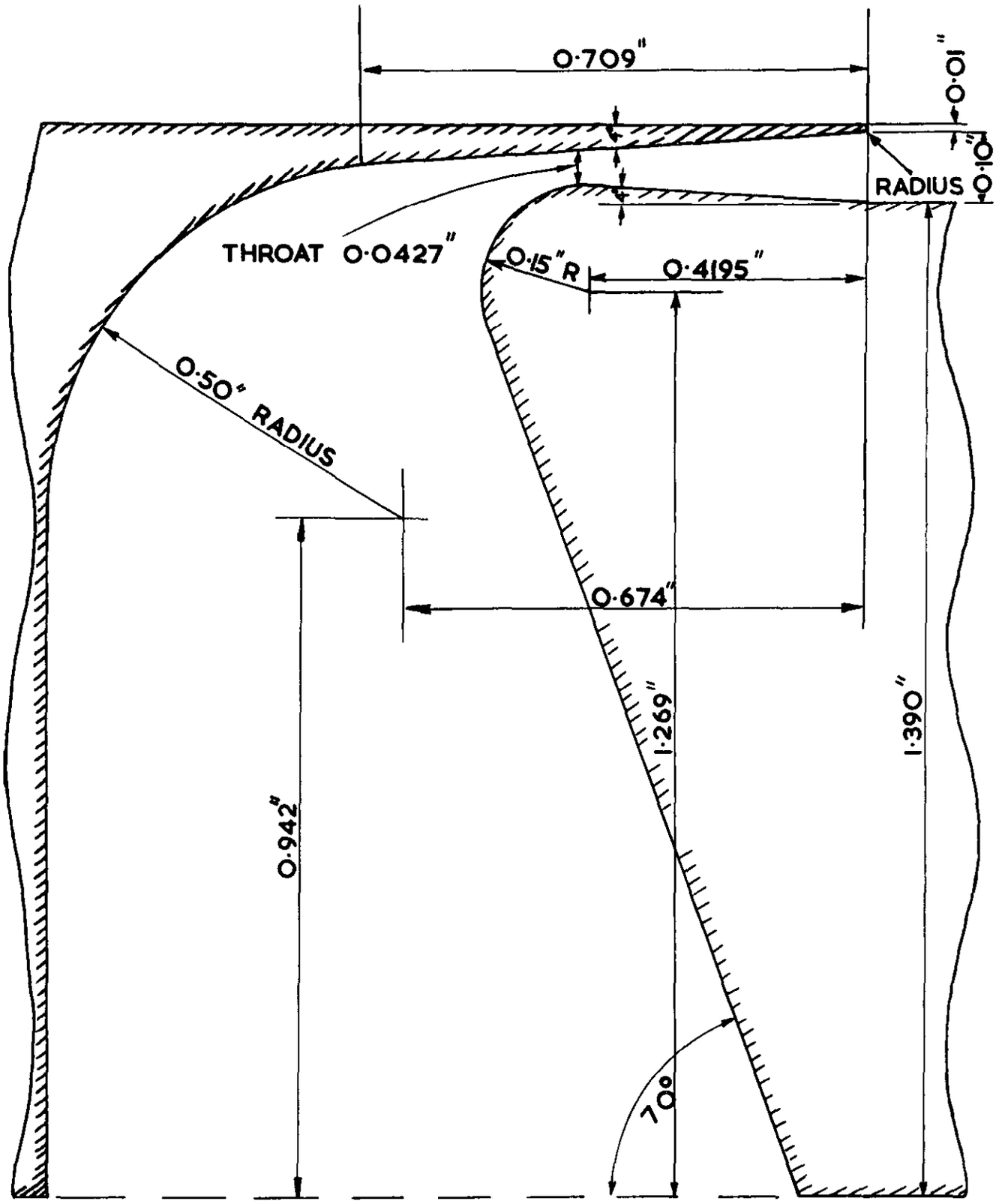

SCALE : 5 X FULL SIZE

INJECTION NOZZLE PROFILE

FIG.5.

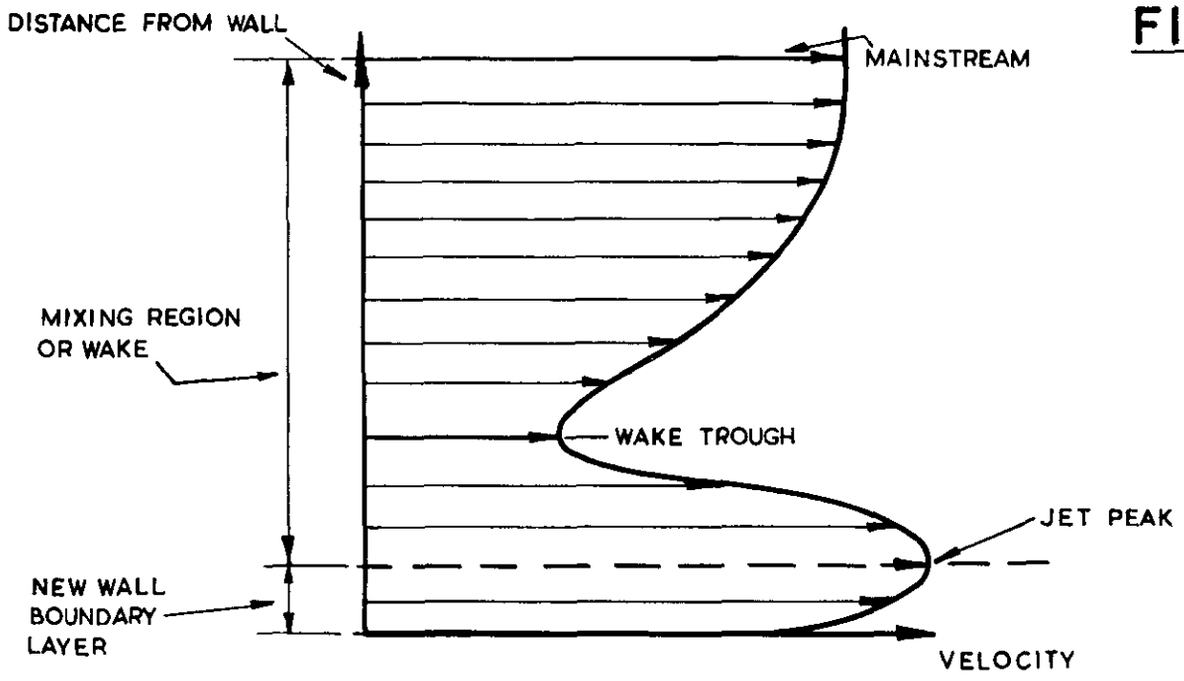

(a) THE VELOCITY PROFILE

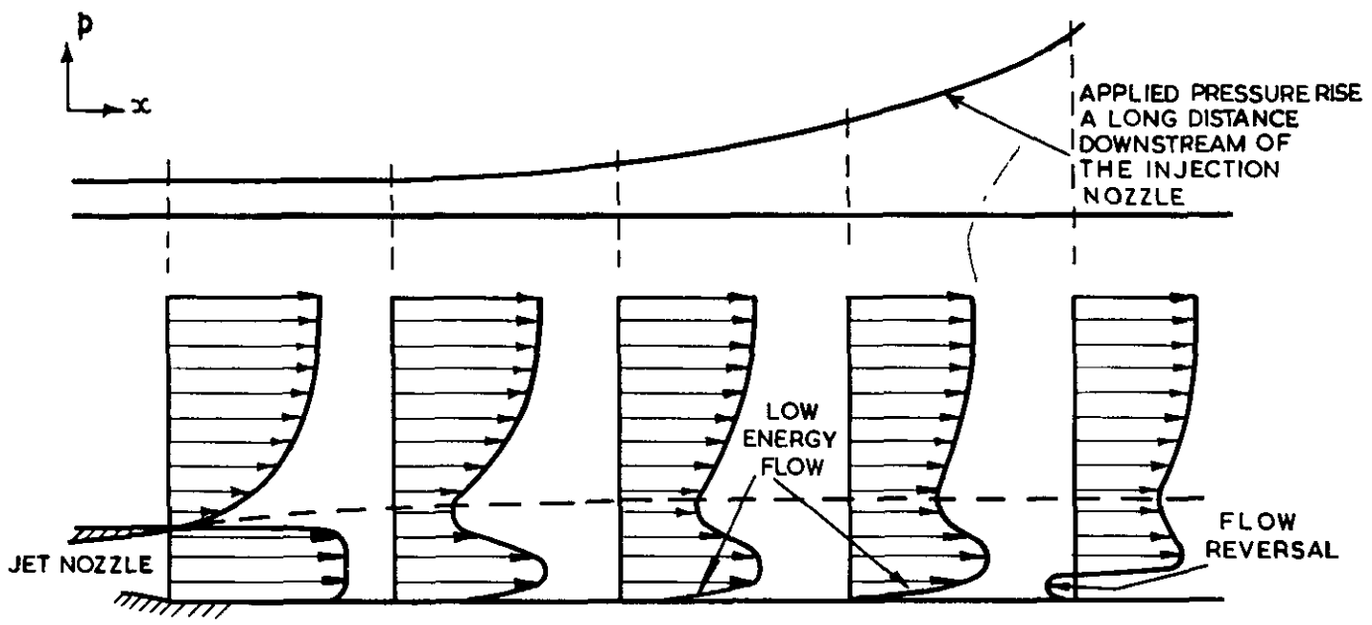

(b) REVERSAL OF THE WALL BOUNDARY LAYER FLOW.

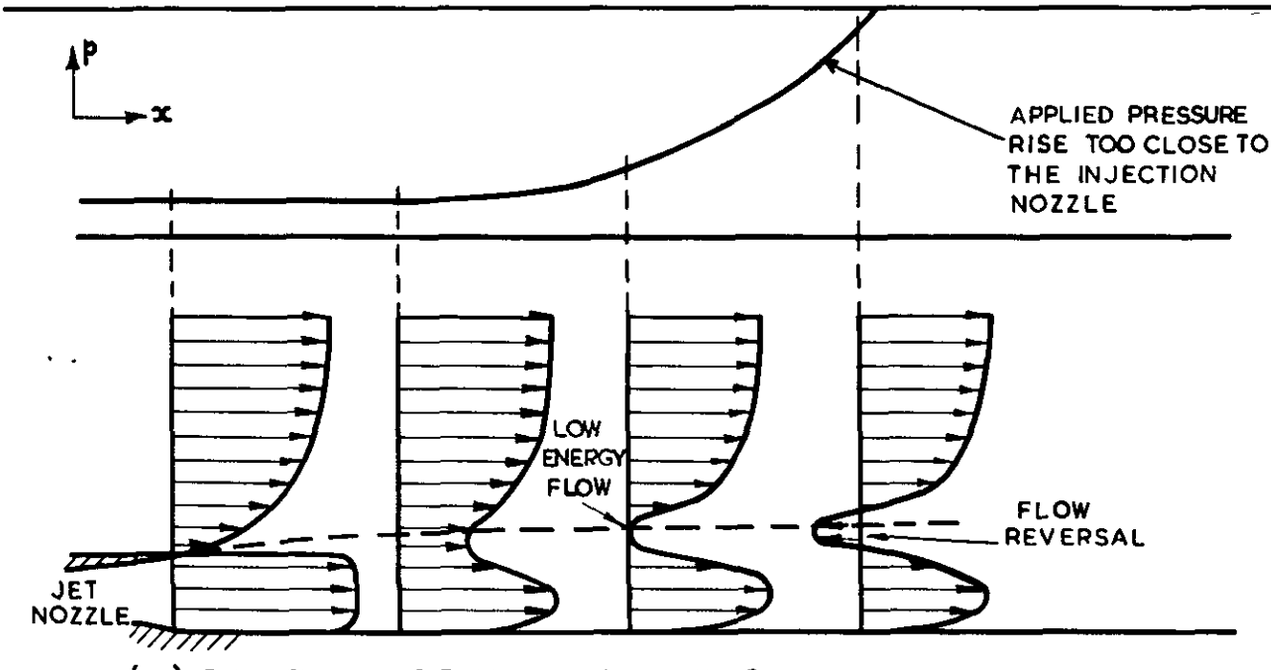

(c) REVERSAL OF THE WAKE FLOW.

FLOW REVERSAL IN THE JET/BOUNDARY LAYER COMBINATION.

FIG. 6

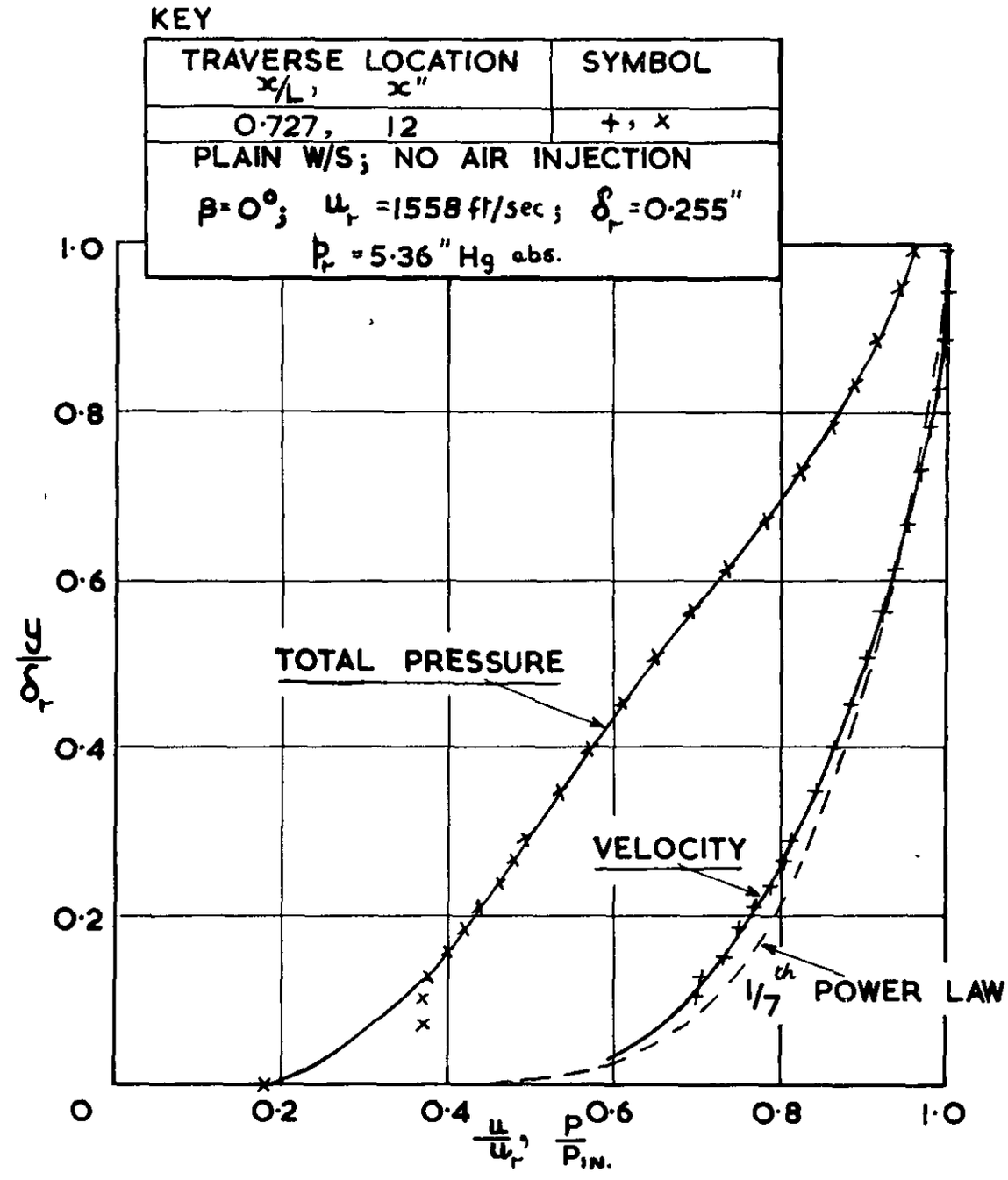

VELOCITY & TOTAL PRESSURE

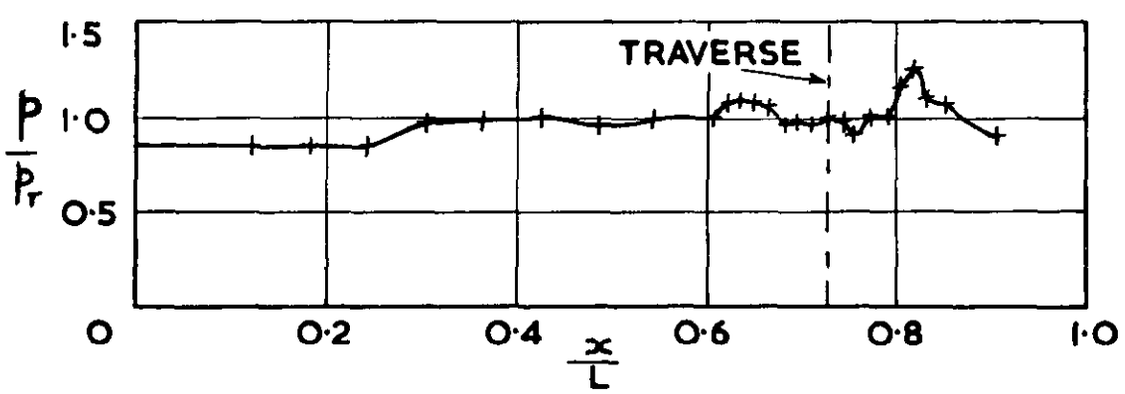

WALL STATIC PRESSURE

REFERENCE PROFILES: THE UNDISTURBED, UNBLOWN BOUNDARY LAYER

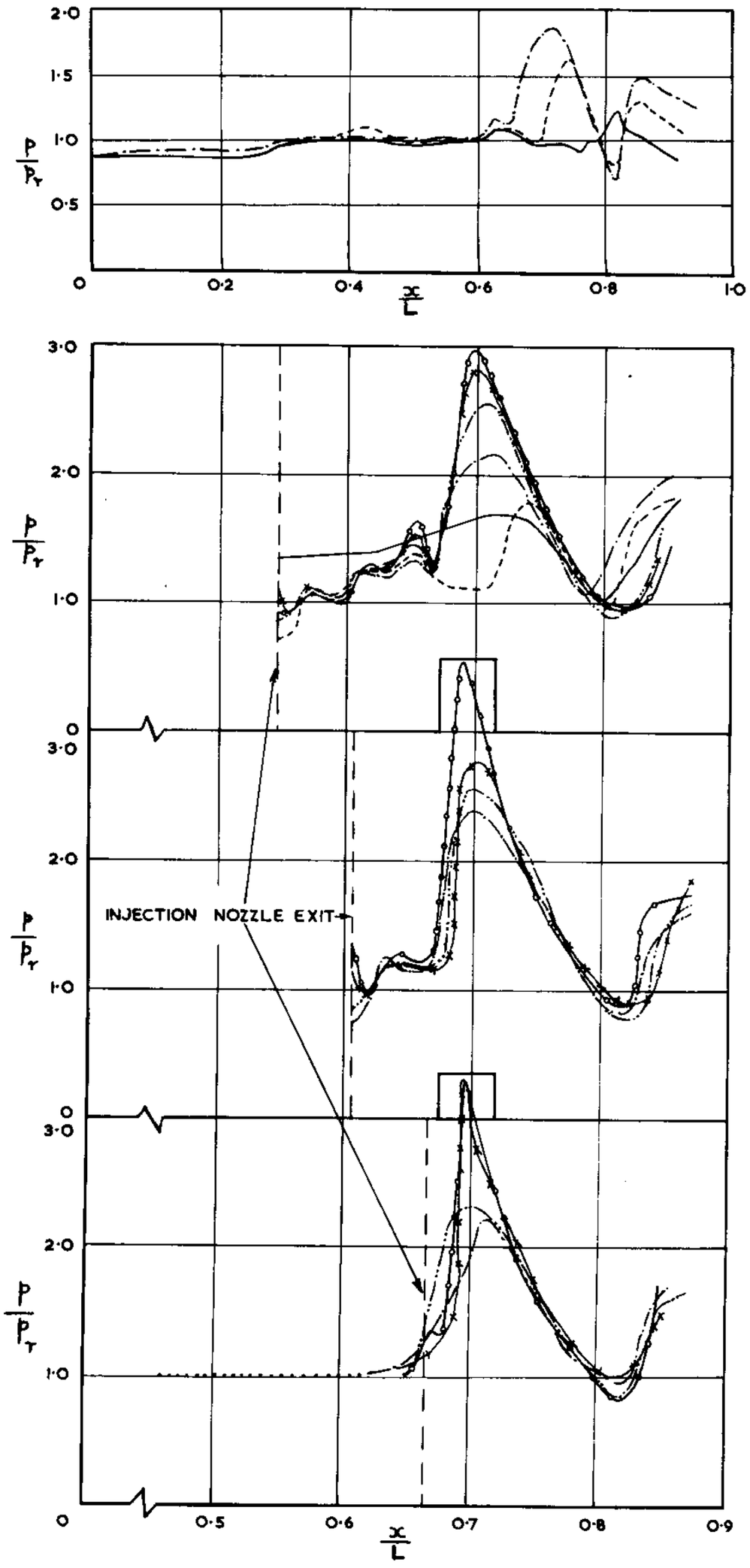

PLAIN WORKING SECTION, WITH NO BLOWING NOZZLE.

———	REFERENCE PROFILE
- - - - -	A_1 WEDGE ANGLE $\beta = 5°$
—·—·—	A_2 WEDGE ANGLE $\beta = 8°$

AIR INJECTION AT x = 9"; 10 ORIGINAL BOUNDARY LAYER THICKNESSES FROM SHOCK PEAK STATIC PRESSURE RISE

TEST	WEDGE ANGLE β°	INJECTION TOTAL PRESSURE / TUNNEL INLET TOTAL PRESSURE
B	6	NO BLOW
C	6	1
D	10·5	1
E	11·5	1·5
F	11·5	2
G	12	2·5

N.B. NOT TEST POINTS

AIR INJECTION AT x = 10"; 6 ORIGINAL BOUNDARY LAYER THICKNESSES FROM SHOCK PEAK STATIC PRESSURE RISE

TEST	WEDGE ANGLE β°	INJECTION TOTAL PRESSURE / TUNNEL INLET TOTAL PRESSURE
M	10	1
N	10·5	2
O_1	11	1·5
O_2	11	2·5

AIR INJECTION AT x = 11"; 2 ORIGINAL BOUNDARY LAYER THICKNESSES FROM SHOCK PEAK STATIC PRESSURE RISE

TEST	WEDGE ANGLE β°	INJECTION TOTAL PRESSURE / TUNNEL INLET TOTAL PRESSURE
P	10	1
Q	10	2
R_1	10	1·5
R_2	10	2·5

WALL STATIC PRESSURE DISTRIBUTIONS.

FIG. 8

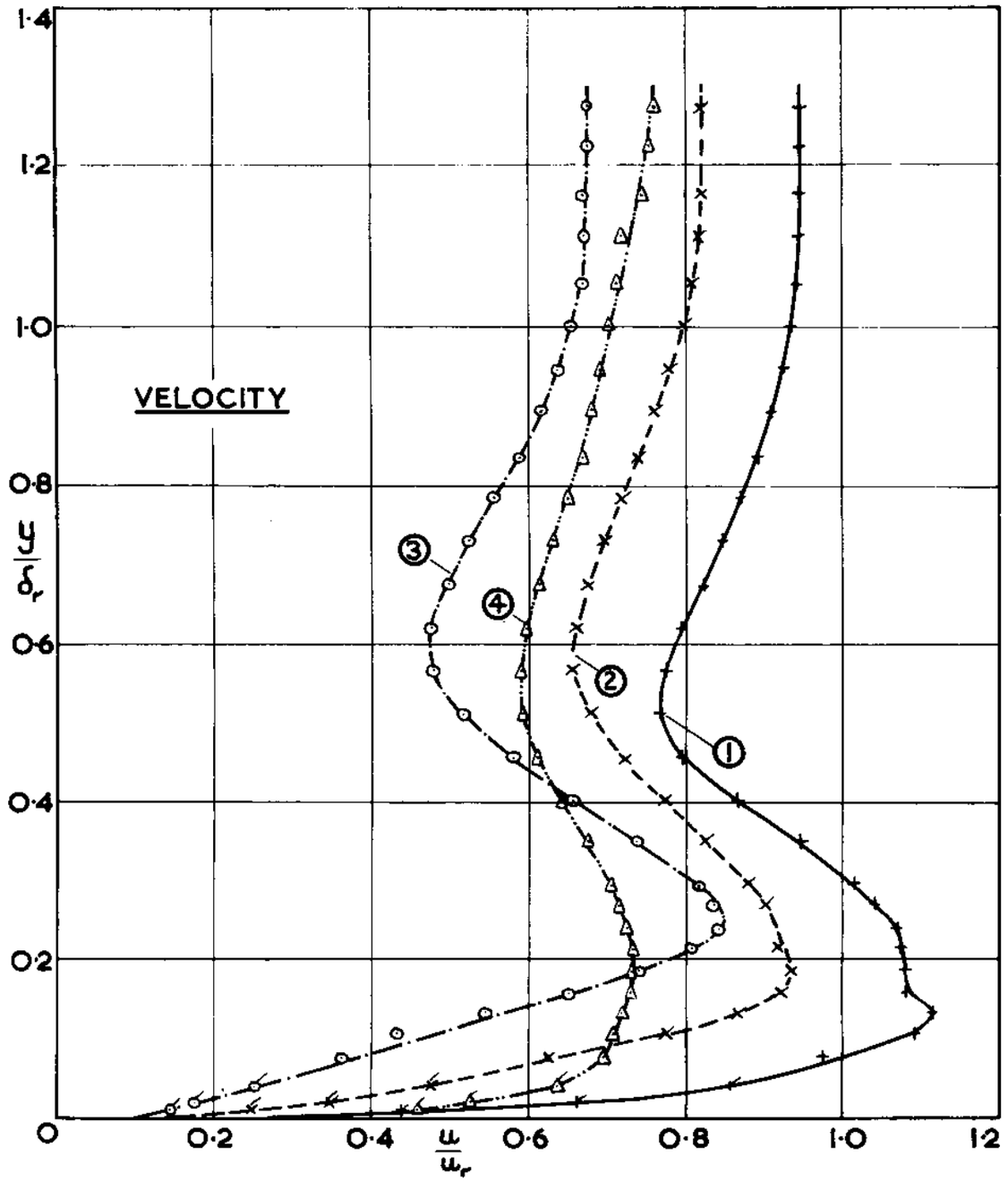

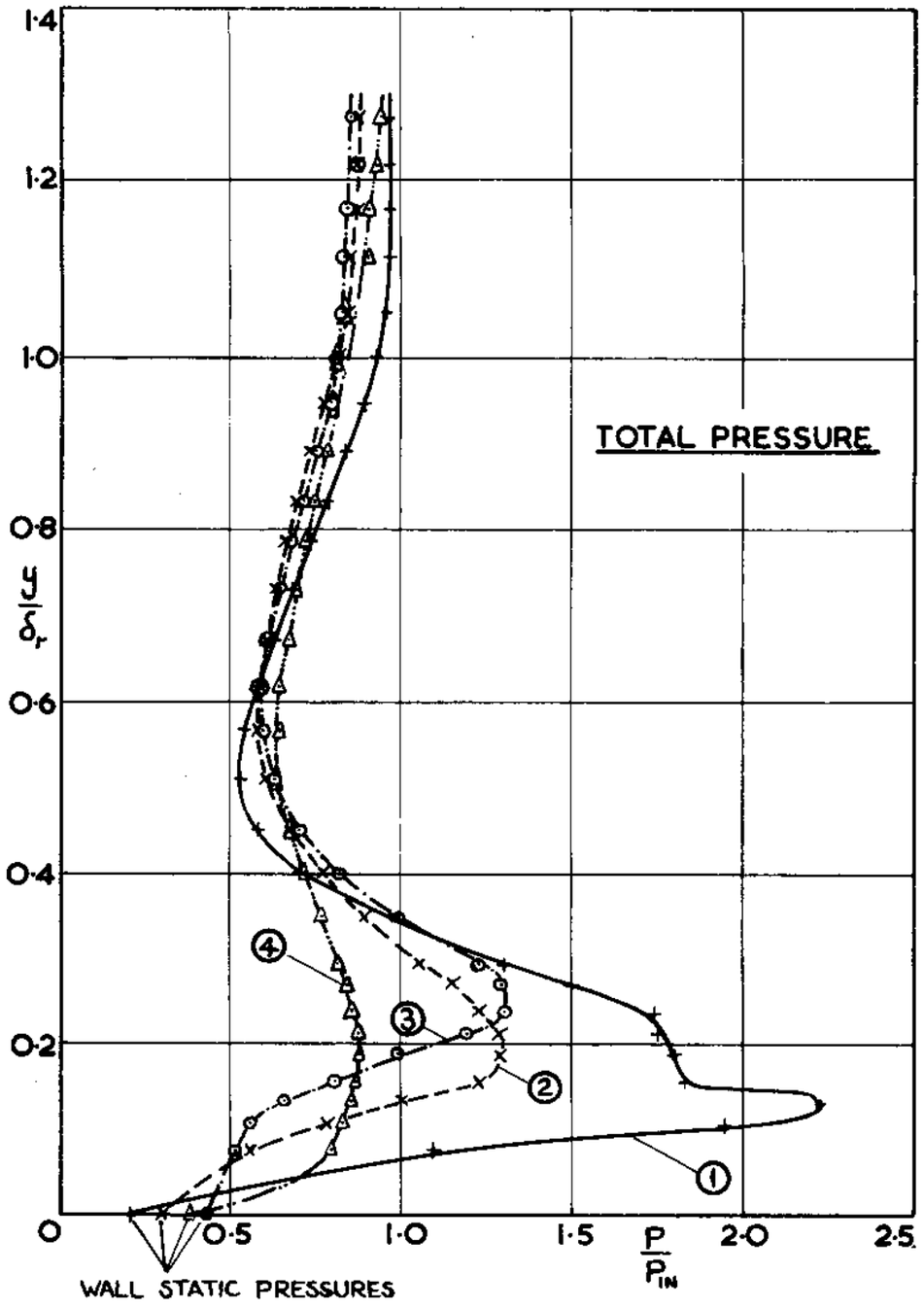

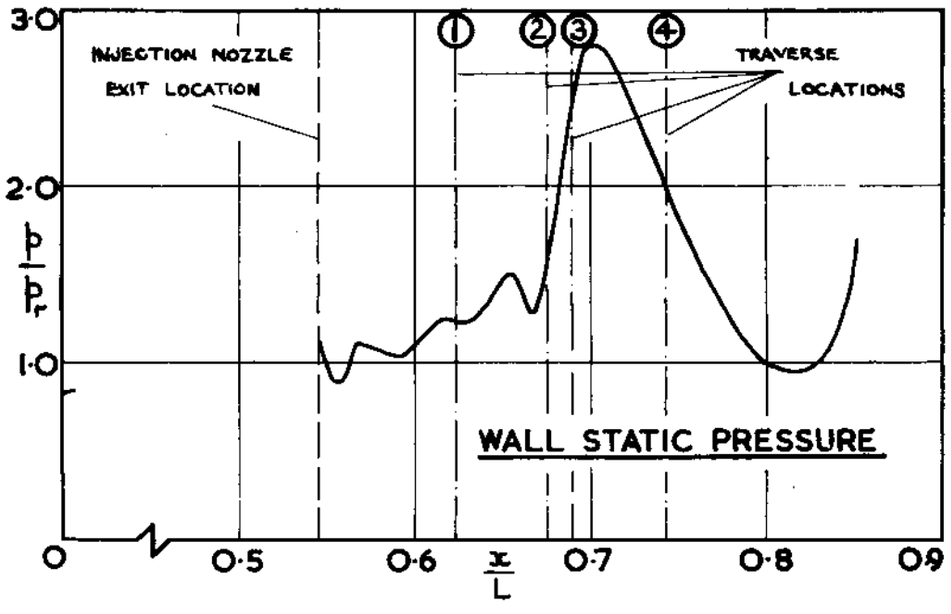

TRAVERSE LOCATION x/L, x"		SYMBOL
1	0·623 , 10·28	—+—
2	0·675 , 11·13	—×—
3	0·689 , 11·37	—○—
4	0·742 , 12·26	—△—

AIR INJECTION AT x = 9": $P_1/P_{IN} \simeq 2$;
β = 11·5° (WEDGE ANGLE)

TEST F : INJECTION AT 2 ATM. ABS. PRESSURE AT x = 9" WITH AN 11·5° WEDGE

FIG. 9

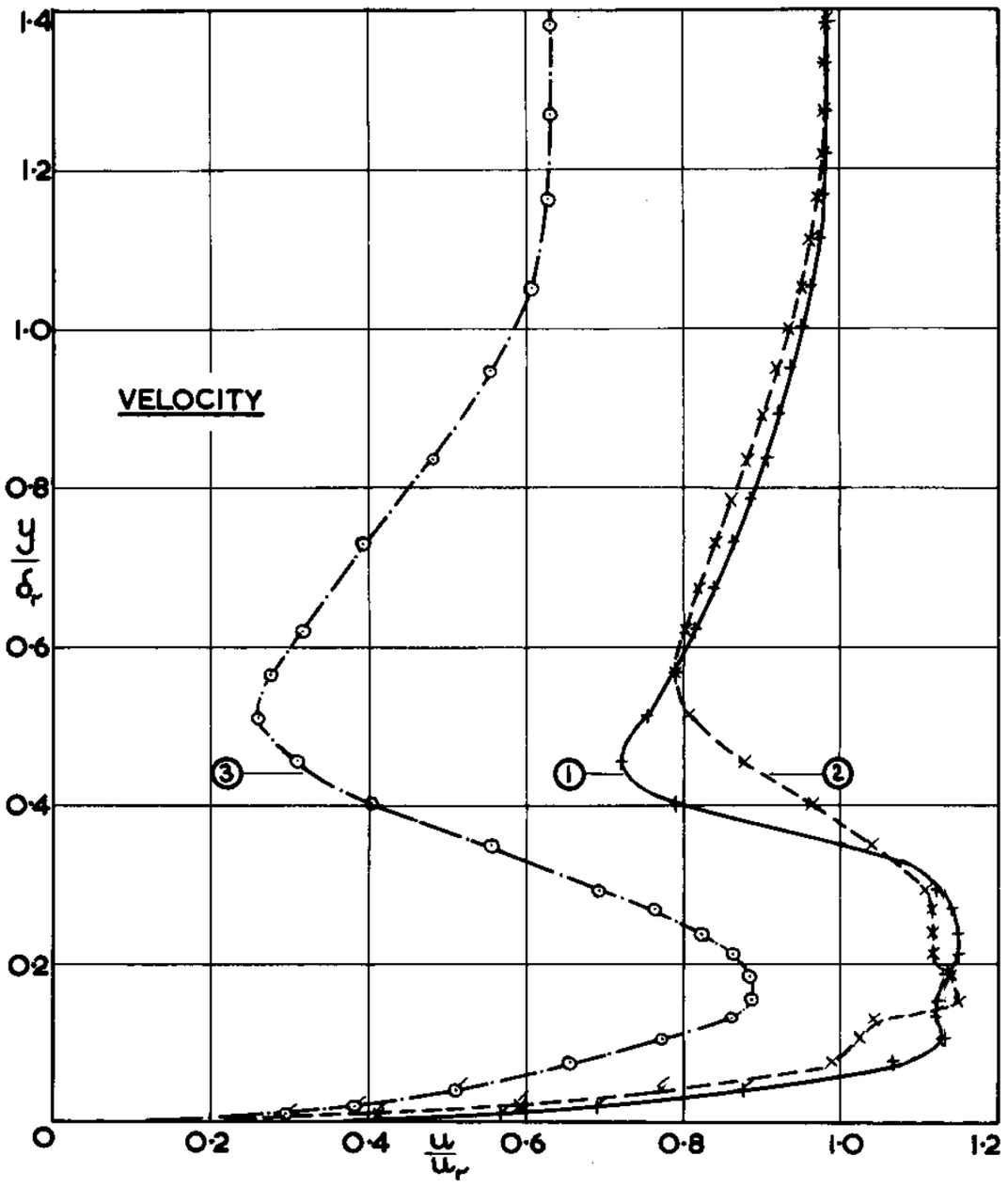

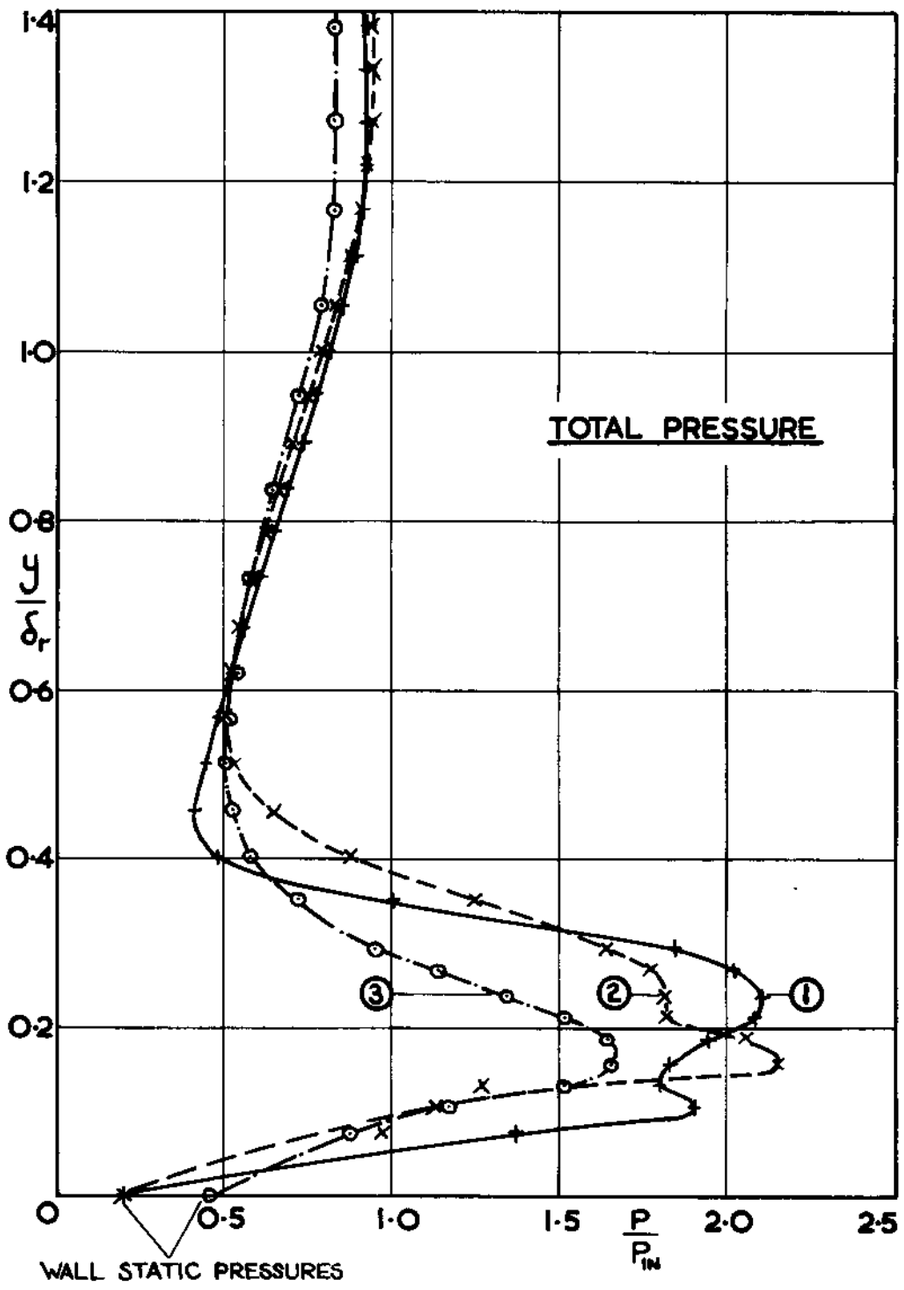

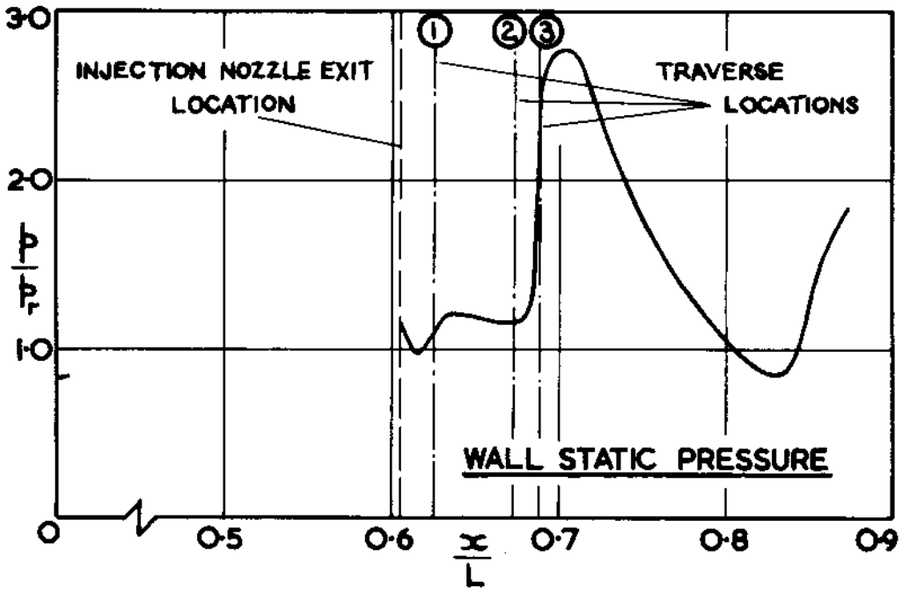

TRAVERSE LOCATION x/L, x''		SYMBOL
1	0·625 , 10·31	—+—
2	0·673 , 11·10	– – × – –
3	0·689 , 11·37	–·–⊙–·–

AIR INJECTION AT $x = 10''$: $P_i/P_{IN} \sim 2$; $\beta = 10·5°$ (WEDGE ANGLE)

TEST N : INJECTION AT 2 ATM. ABS. PRESSURE AT $x = 10''$ WITH A 10·5° WEDGE

FIG. 10

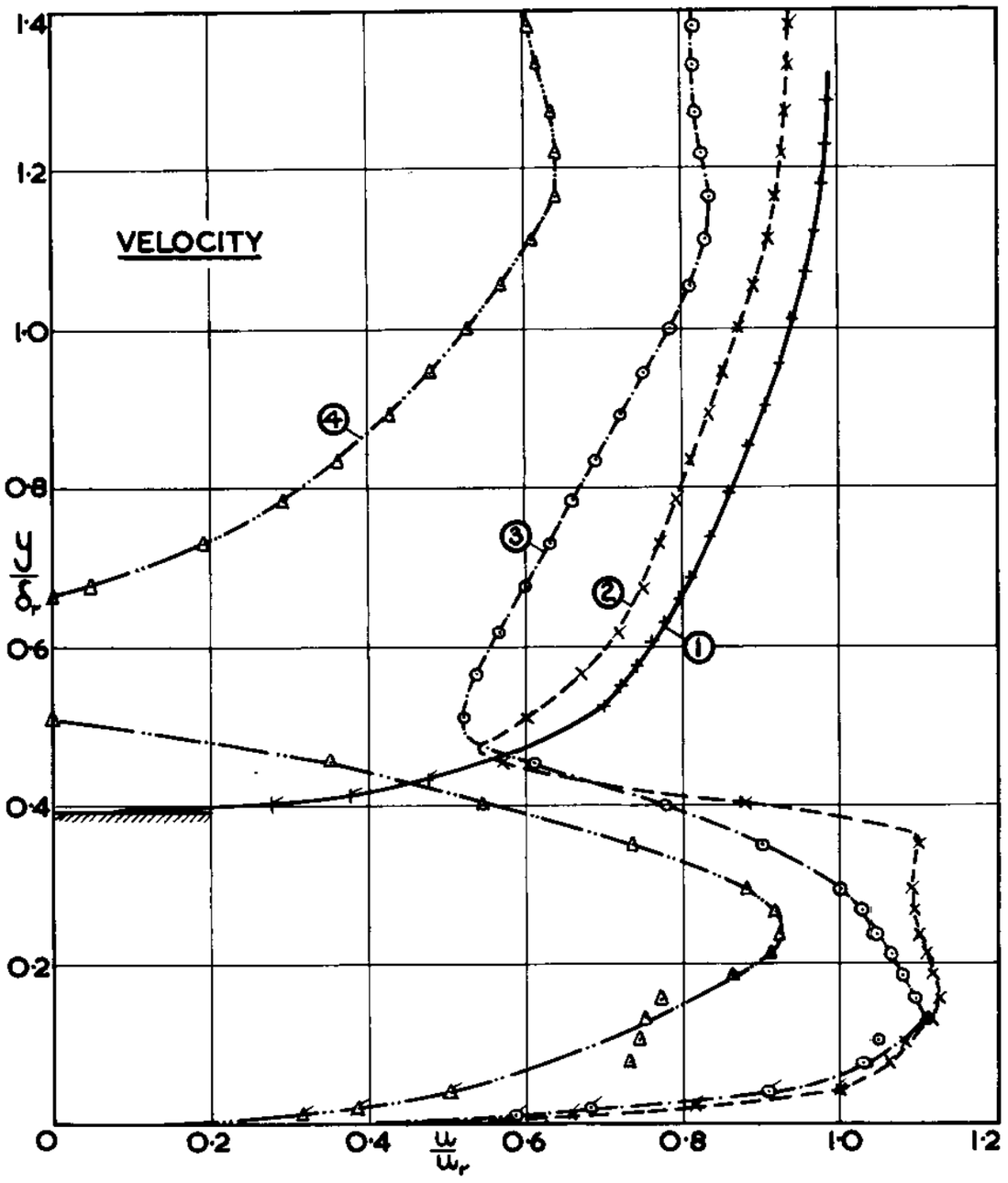

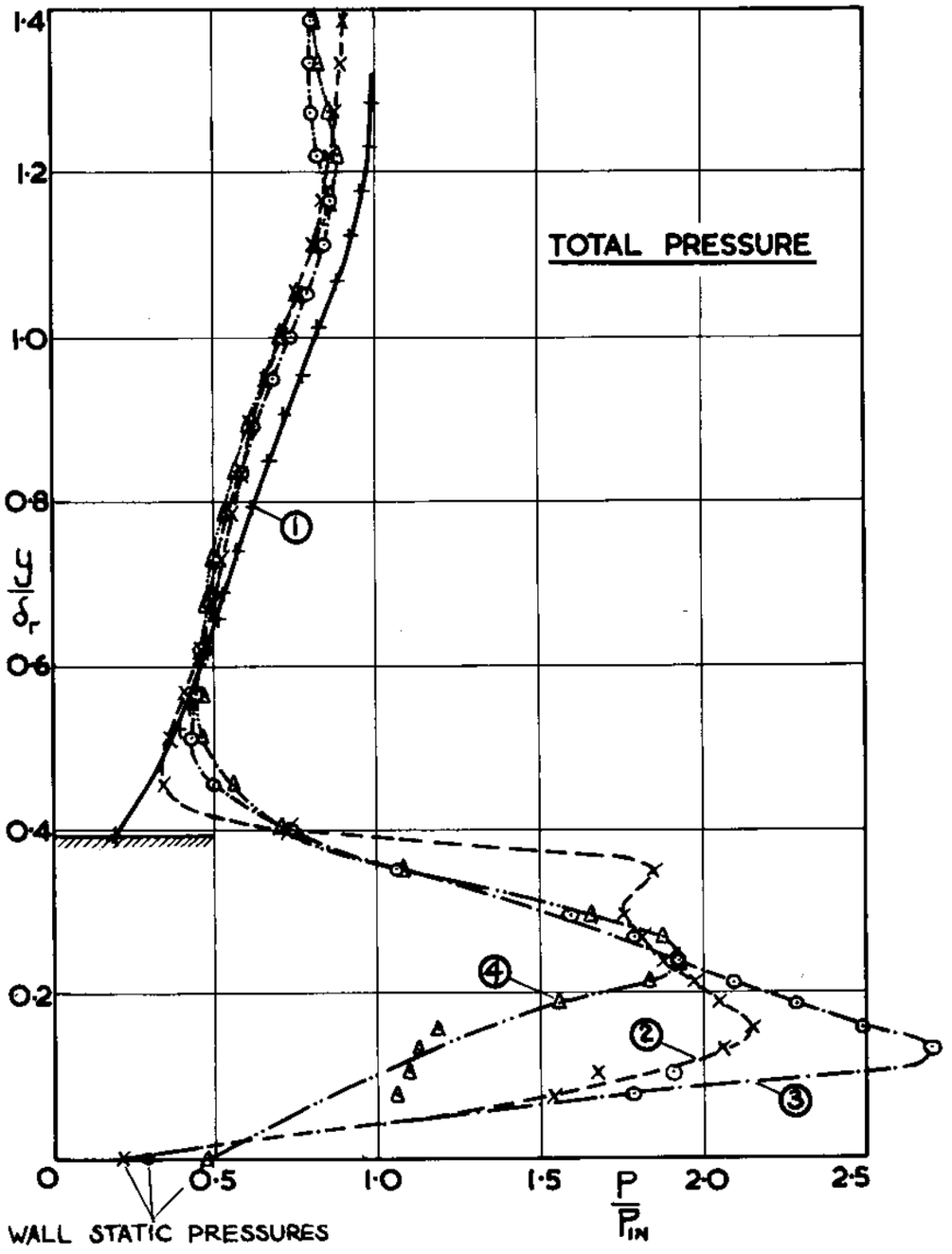

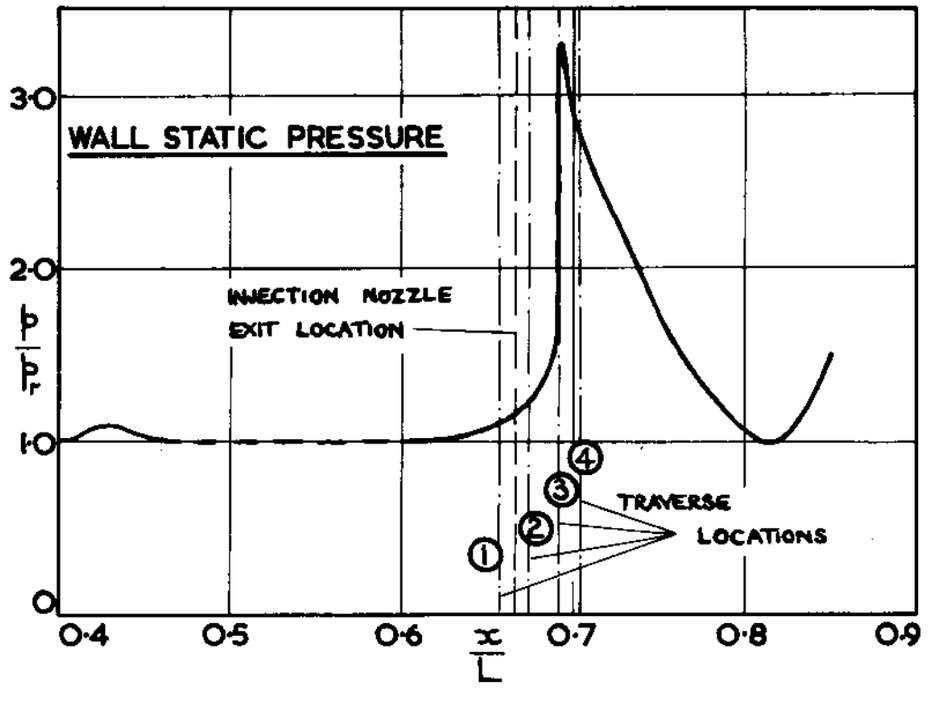

TRAVERSE LOCATION x/L, x"		SYMBOL
1	0·657, 10·84	—+—
2	0·673, 11·10	– – X – –
3	0·691, 11·40	—·—⊙—·—
4	0·709, 11·60	—·—Δ—·—

AIR INJECTION AT x=11": $P_t/P_{IN} \simeq 2$; β=10°(WEDGE ANGLE)

TEST Q : INJECTION AT 2 ATM. ABS. PRESSURE AT x=11" WITH A 10° WEDGE

FIG. 11

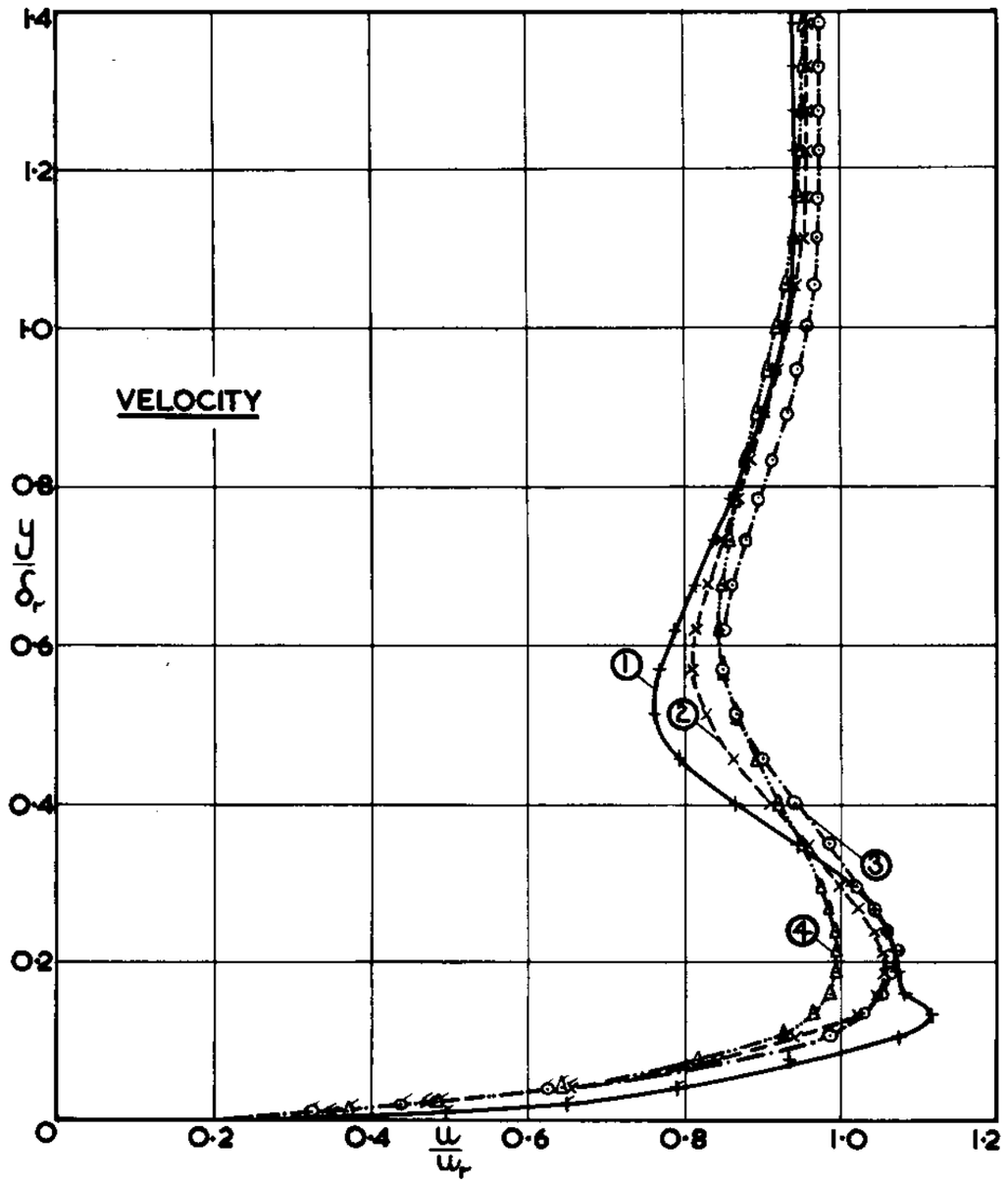

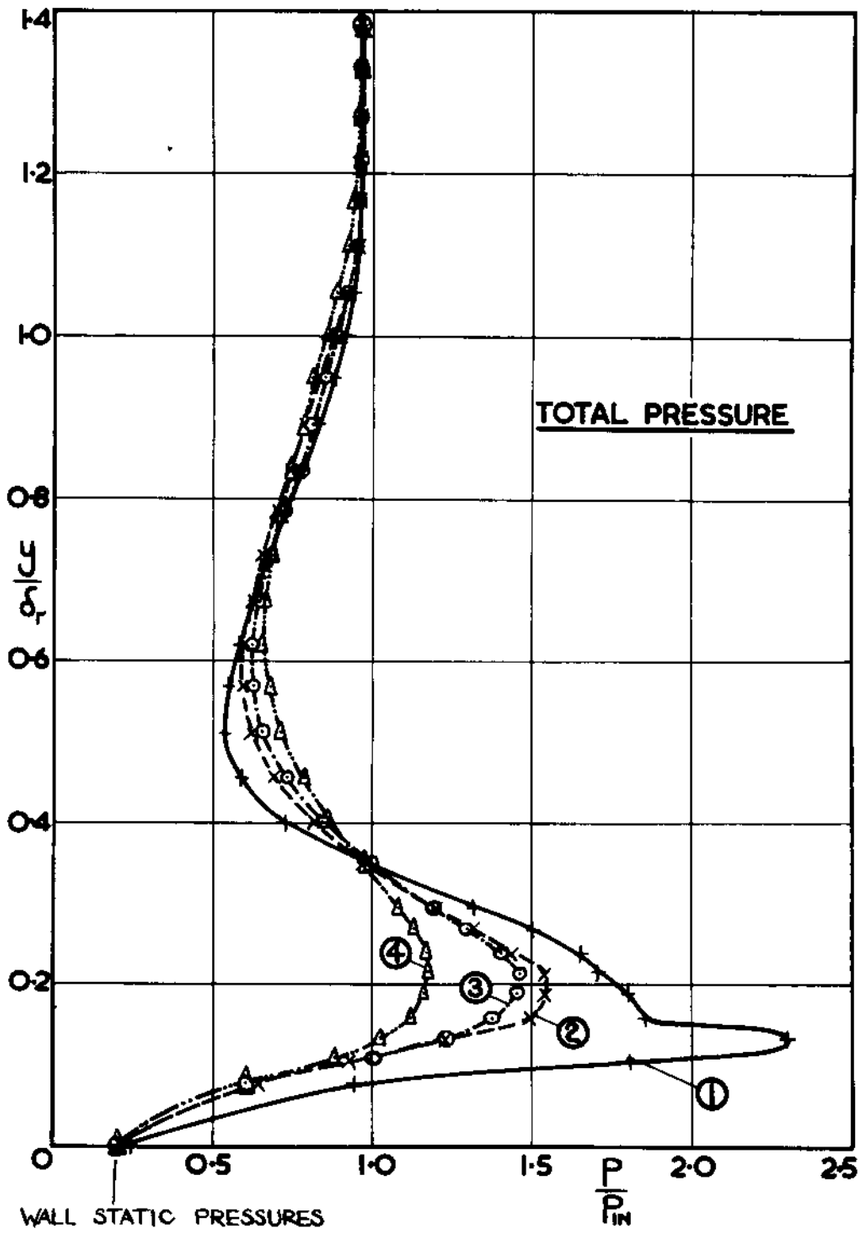

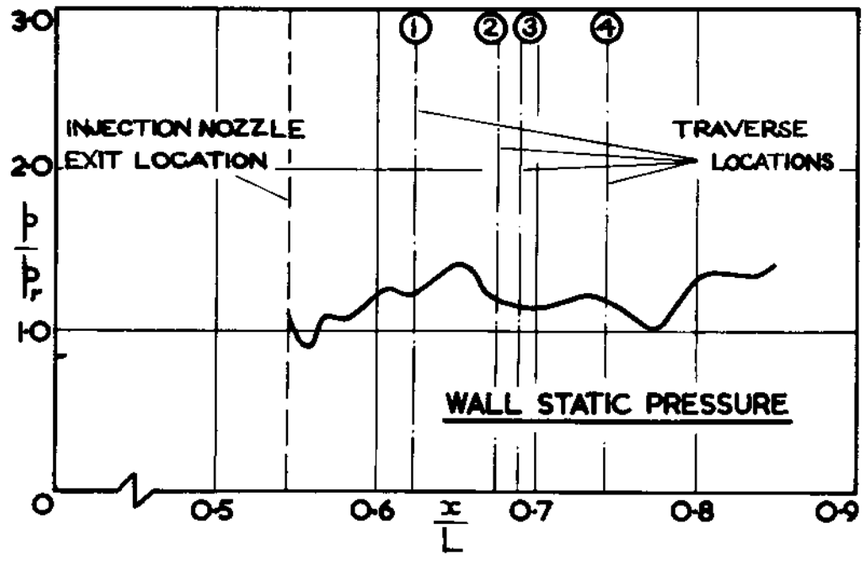

TRAVERSE LOCATION x/L, x"		SYMBOL
1	0·623, 10·28	—+—
2	0·675, 11·18	— — x — —
3	0·689, 11·37	—·—○—·—
4	0·742, 12·25	—·—△—·—
AIR INJECTION AT x=9": $P_I/P_{IN} \simeq 2$; β=0° (WEDGE ANGLE).		

TEST K: INJECTION AT 2 ATM. ABS. PRESSURE AT x=9" WITH A 0° WEDGE.

FIG. 12

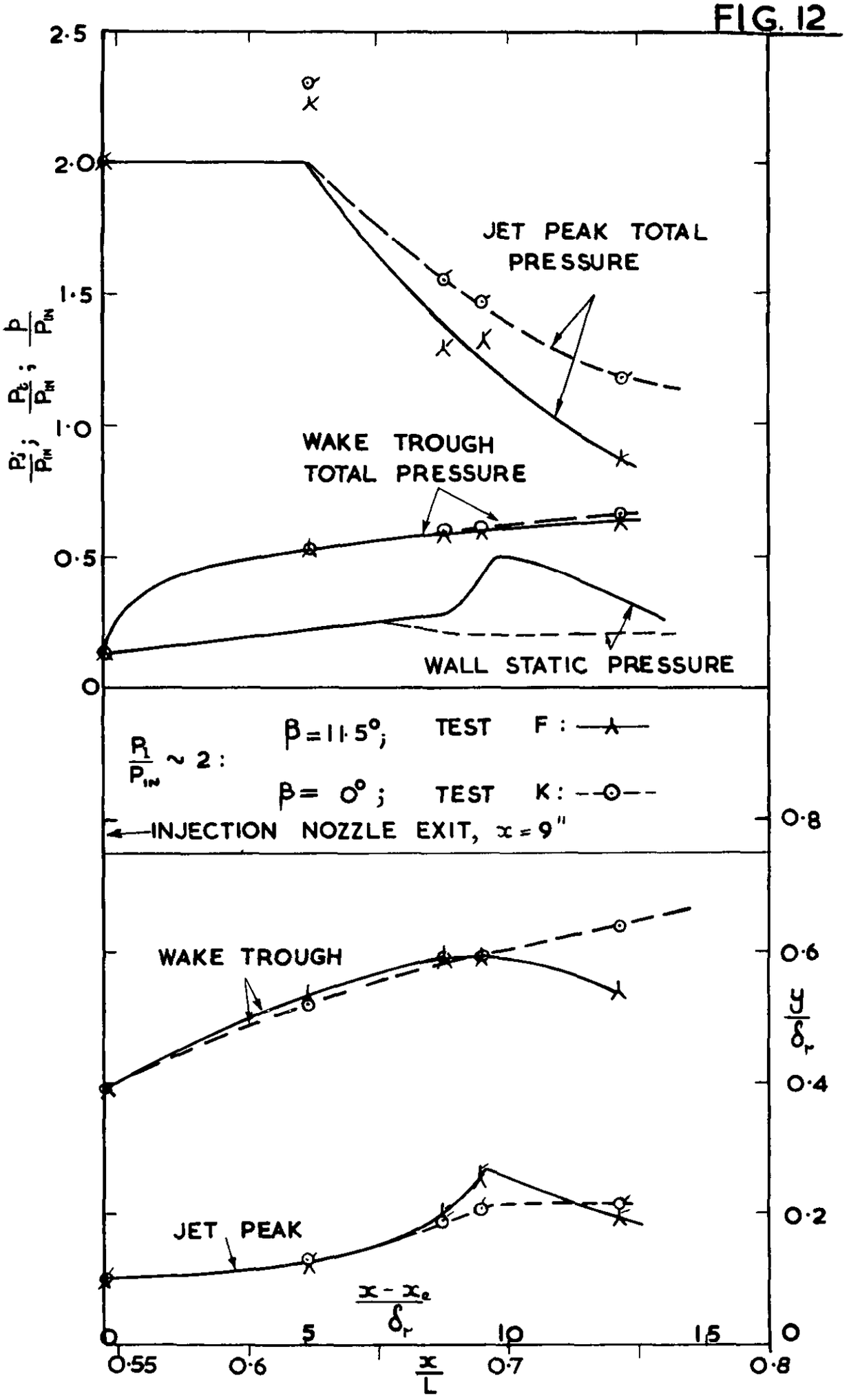

CHARACTERISTICS OF THE WAKE TROUGH AND JET PEAK: TESTS F & K COMPARED

(LENGTH OF MIXING REGION = 10 δ_r)

FIG. 13

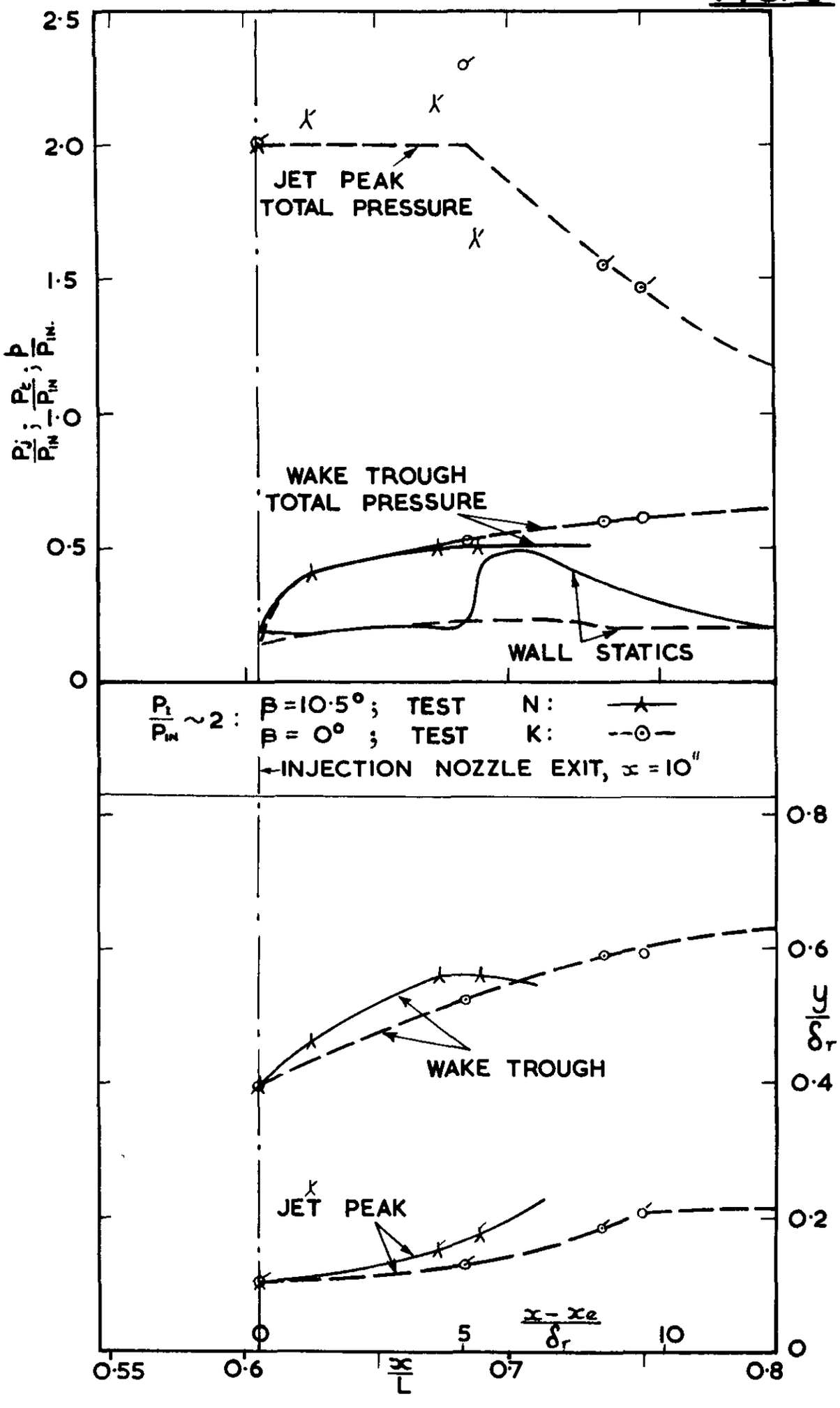

CHARACTERISTICS OF THE WAKE TROUGH AND JET PEAK: TESTS N & K COMPARED

(LENGTH OF MIXING REGION = $6\delta_r$)

FIG. 14

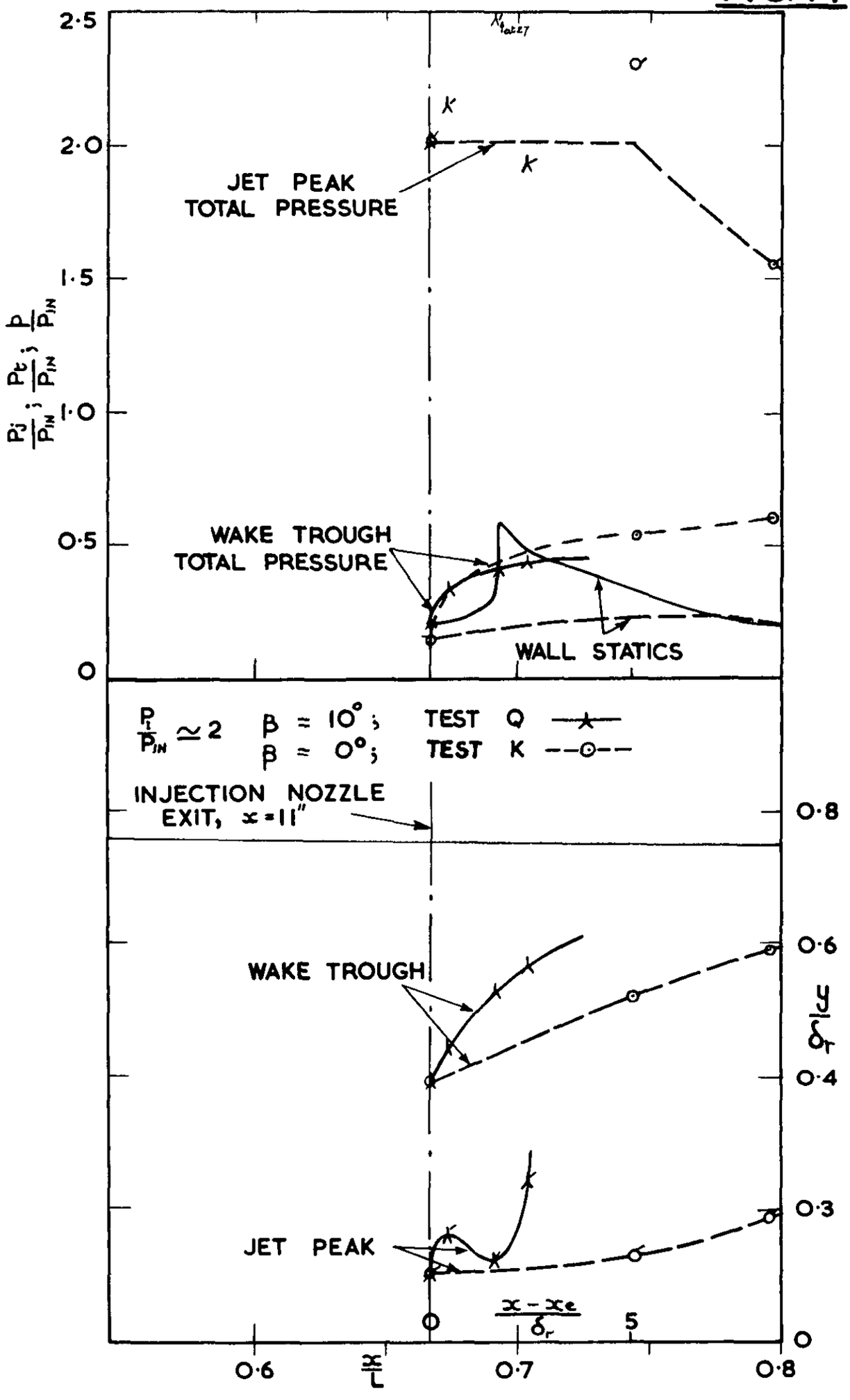

CHARACTERISTICS OF THE WAKE TROUGH AND JET PEAK: TESTS Q & K COMPARED

(LENGTH OF MIXING REGION = 2 δ_T)

FIG. 15

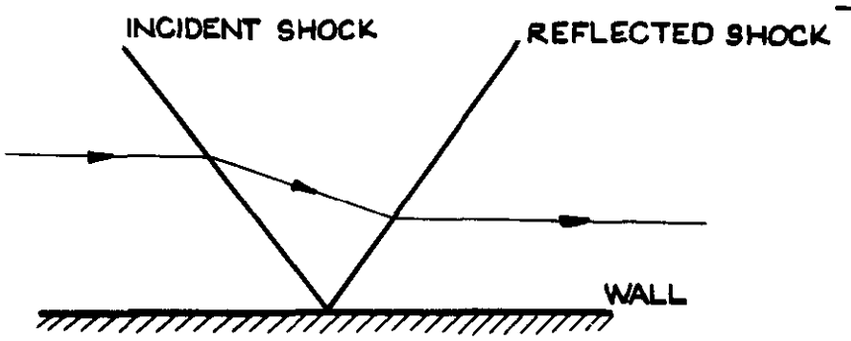

(a) REGULAR REFLECTION OF OBLIQUE SHOCK; NO BOUNDARY LAYER

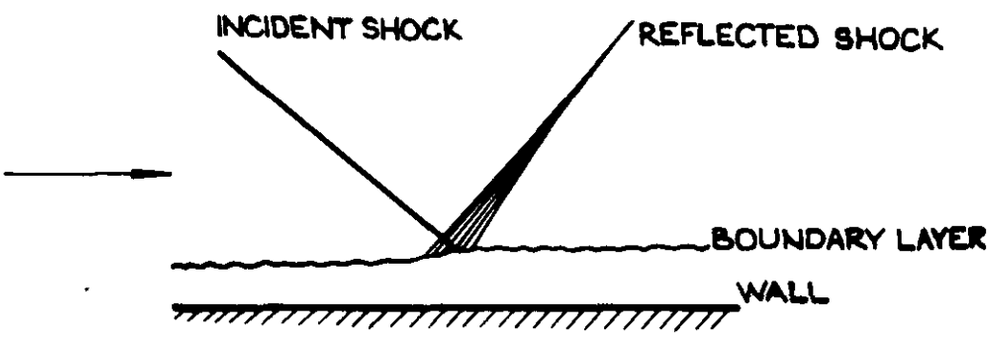

(b) REFLECTION OF OBLIQUE SHOCK; WITH SUPERSONIC TURBULENT BOUNDARY LAYER.

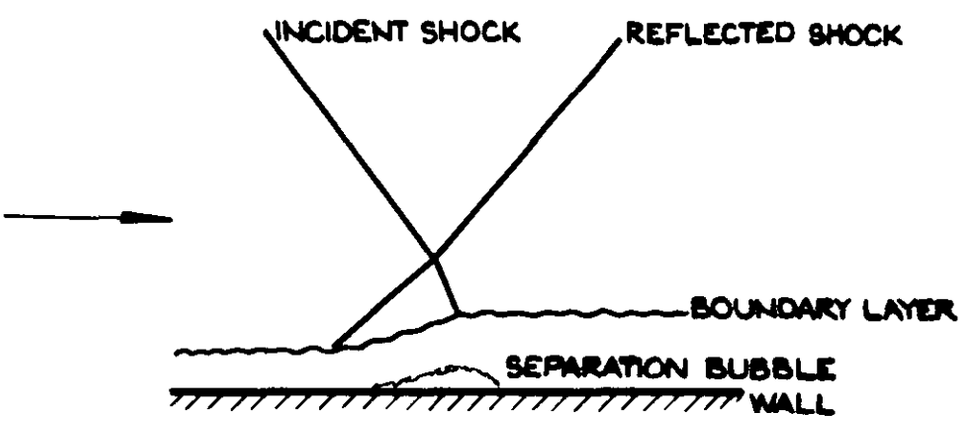

(c) REFLECTION OF STRONGER OBLIQUE SHOCK; WITH SUPERSONIC TURBULENT BOUNDARY LAYER.

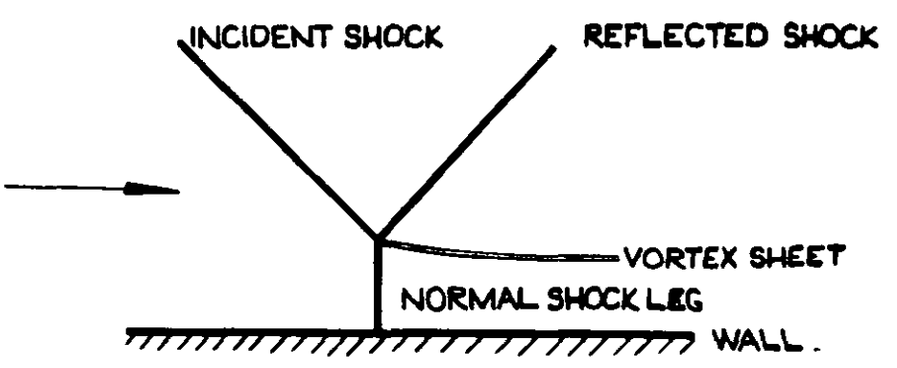

(d) MACH REFLECTION.

REFLECTION OF OBLIQUE SHOCK WAVE

FIG. 16

FLOW DIRECTION, KNIFE EDGE HORIZONTAL

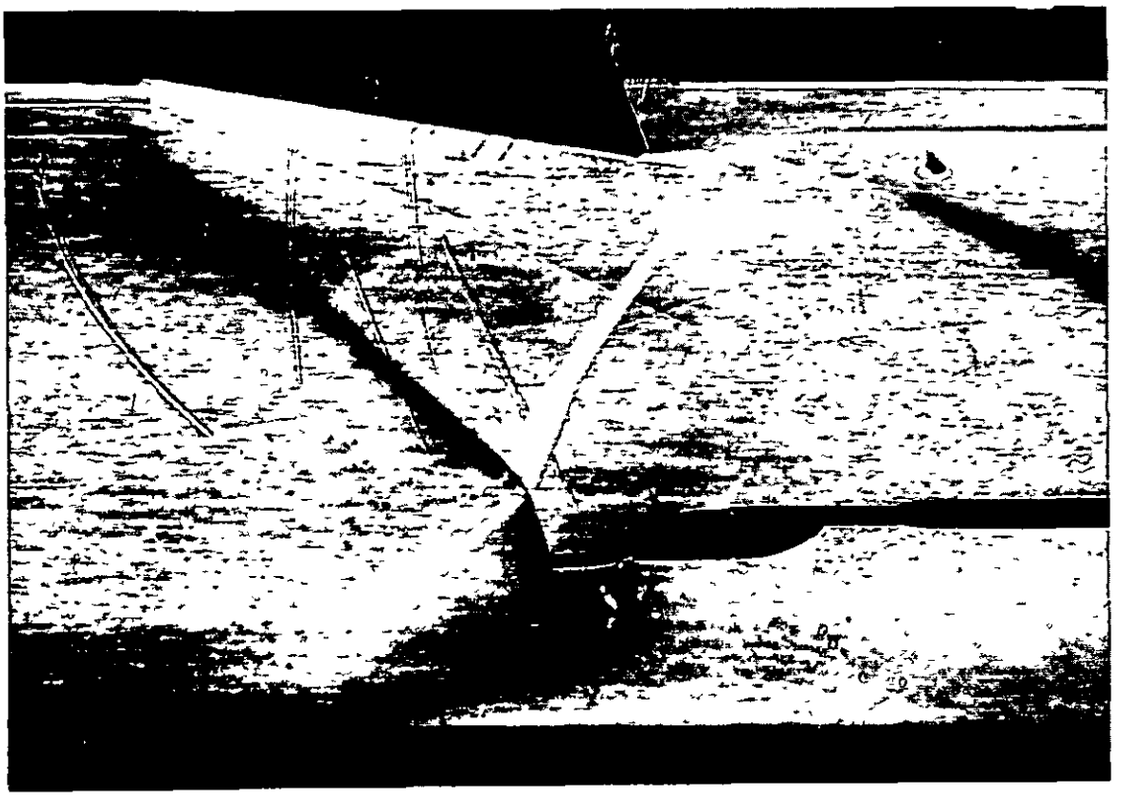

(a) TEST A_2, PLAIN WORKING SECTION, $\beta = 8^\circ$

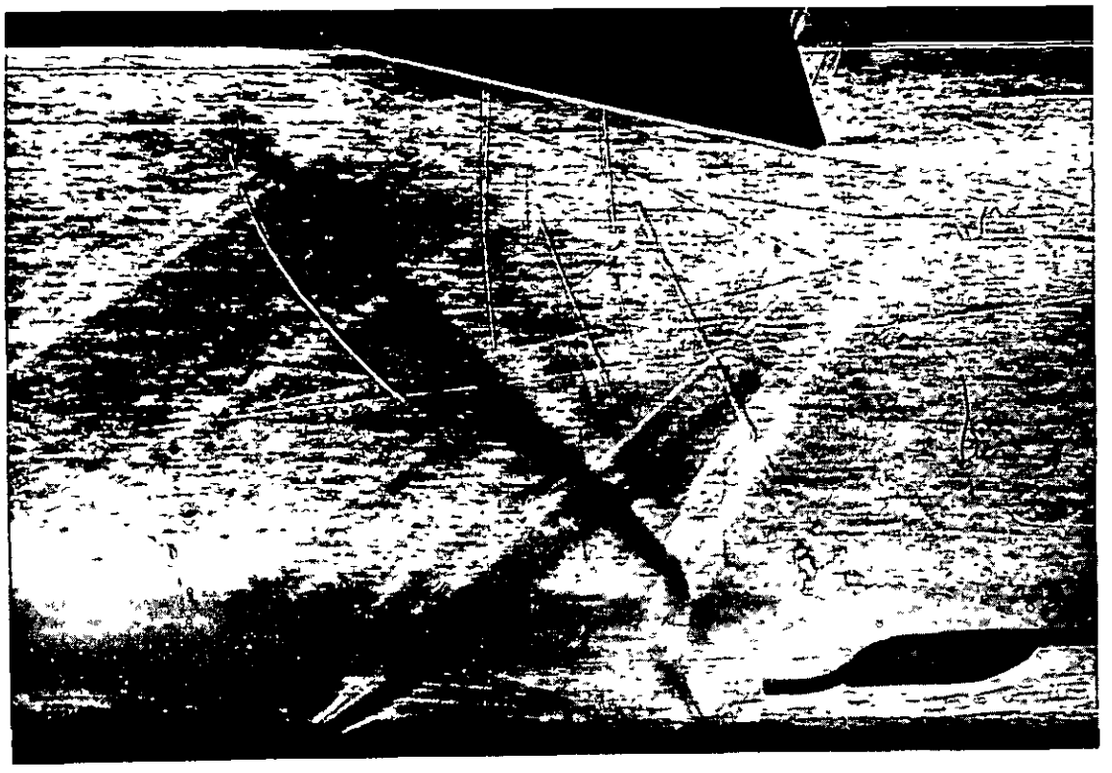

(b) TEST G, WITH INJECTION, $P_I/P_{IN} \sim 2.5$ $\beta = 12^\circ$

THE INJECTION SLOT IS UPSTREAM OF THE POINT P

EXAMPLES OF THE FLOW PATTERNS.

FIG.17.

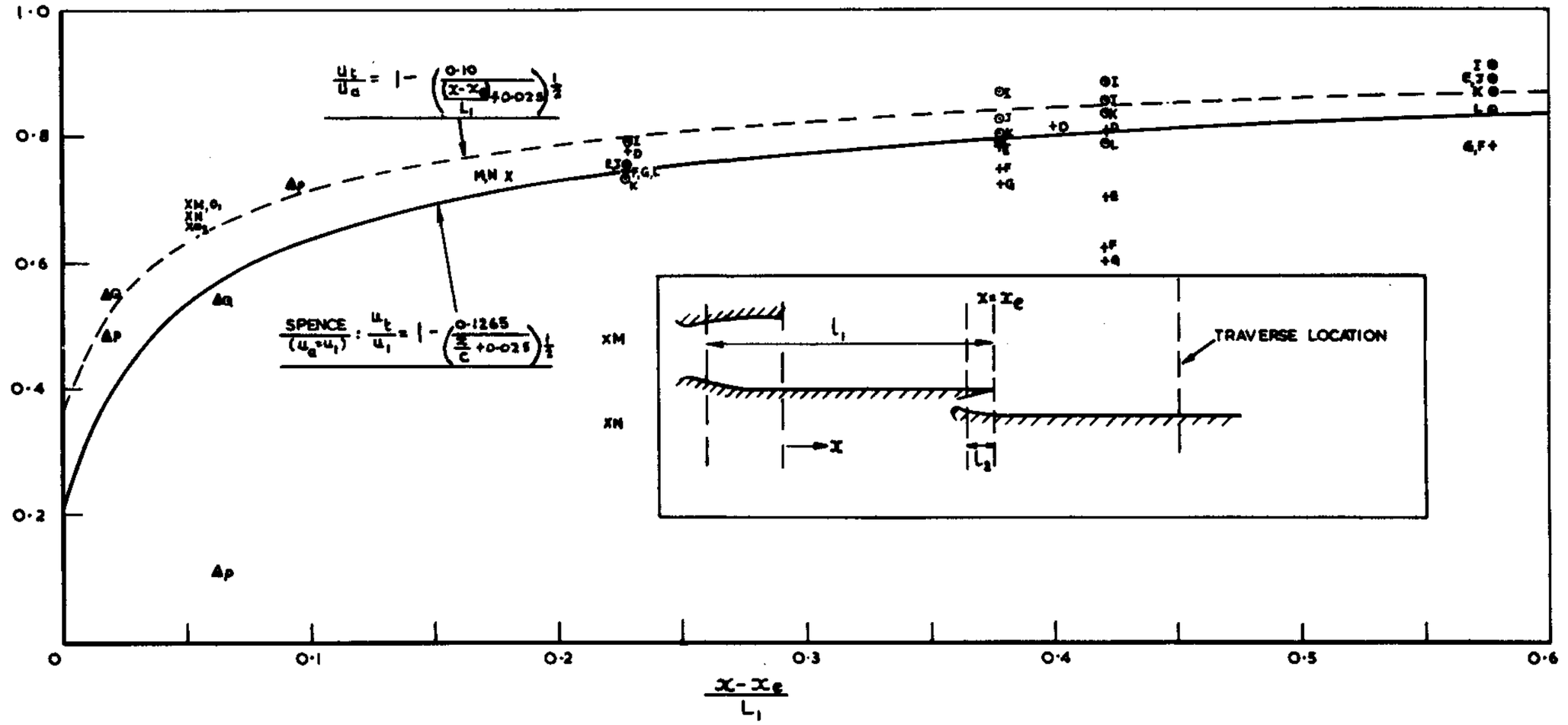

VELOCITY ON WAKE CENTRE-LINE: $u_a = \frac{u_1 + u_j}{2}$

FIG 18

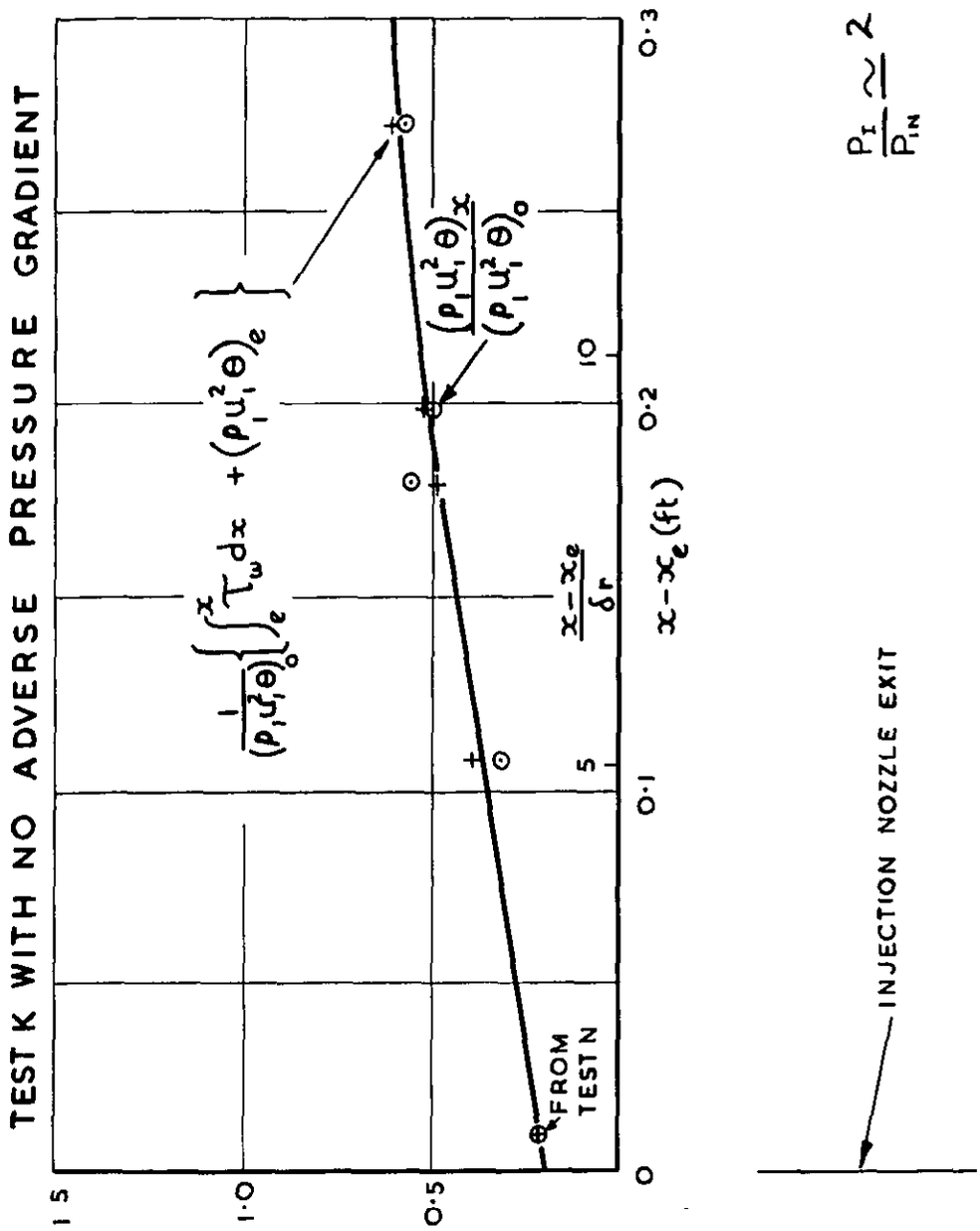

THE MOMENTUM INTEGRAL EQUATION

FIG. 19

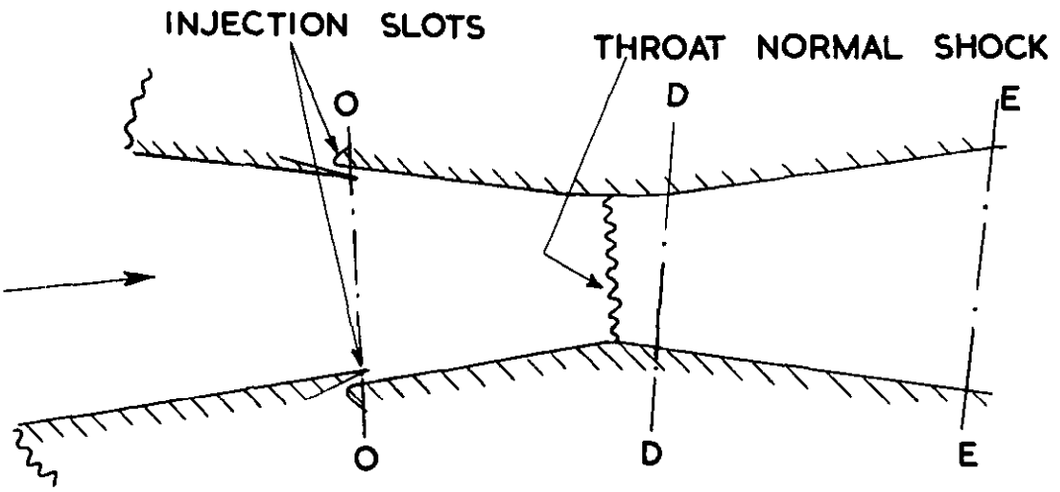

a) SCHEMATIC REPRESENTATION OF A SUPERSONIC AIR INTAKE WITH INJECTION BOUNDARY LAYER CONTROL UPSTREAM OF THE THROAT.

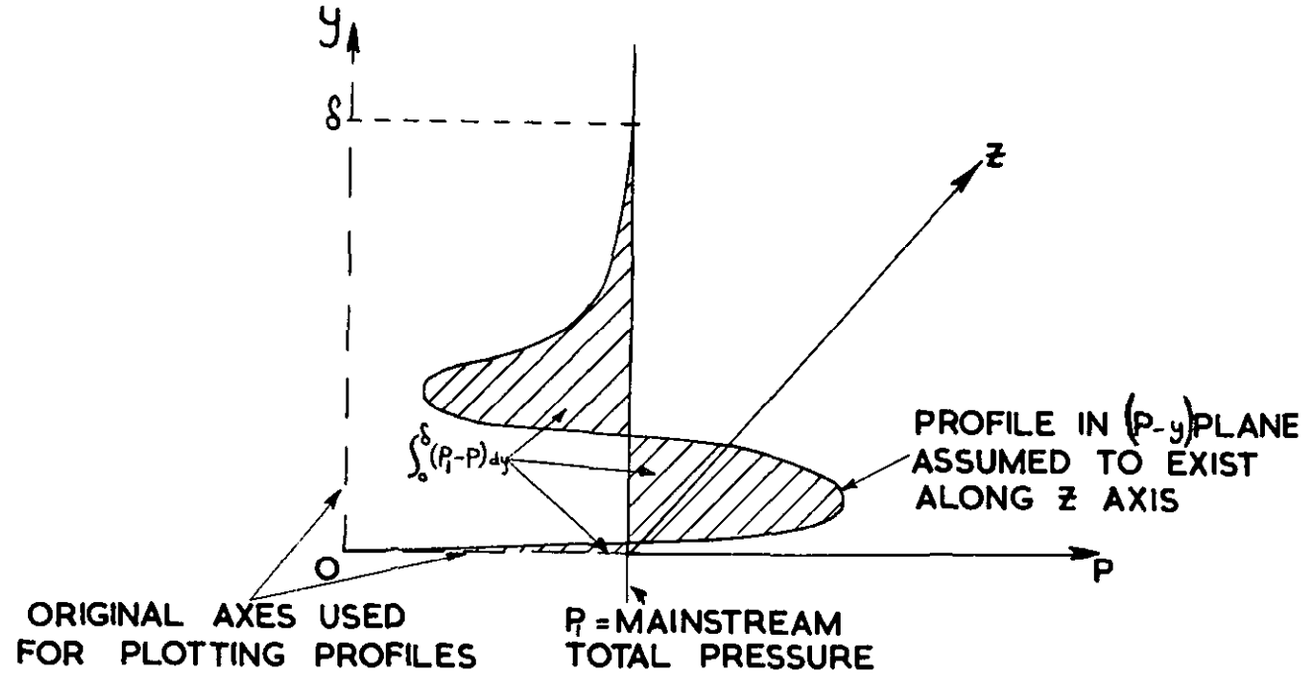

b) SHADED AREAS REPRESENTING THOSE USED IN THE CALCULATION OF THE AREA TOTAL PRESSURE DEFICIENCY.

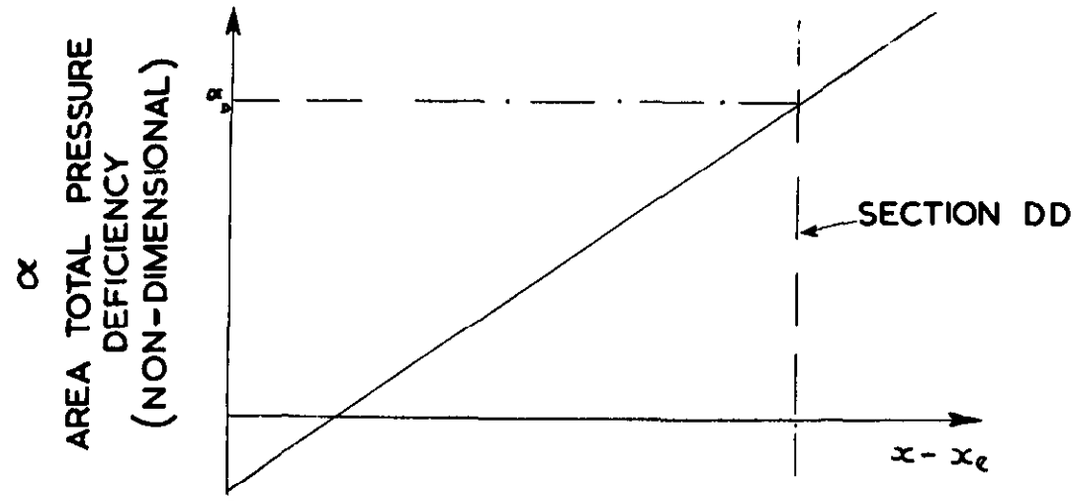

c) AREA TOTAL PRESSURE DEFICIENCY WITH DISTANCE DOWNSTREAM OF INJECTION POINT. $\alpha = \int_0^\delta (P_1-P)\,dy \,/\, \int_0^{\delta_0} (P_1-P)\,dy_0$

MEAN TOTAL PRESSURE RECOVERY OF AN INTAKE WITH INJECTION BOUNDARY LAYER CONTROL.

FIG. 20

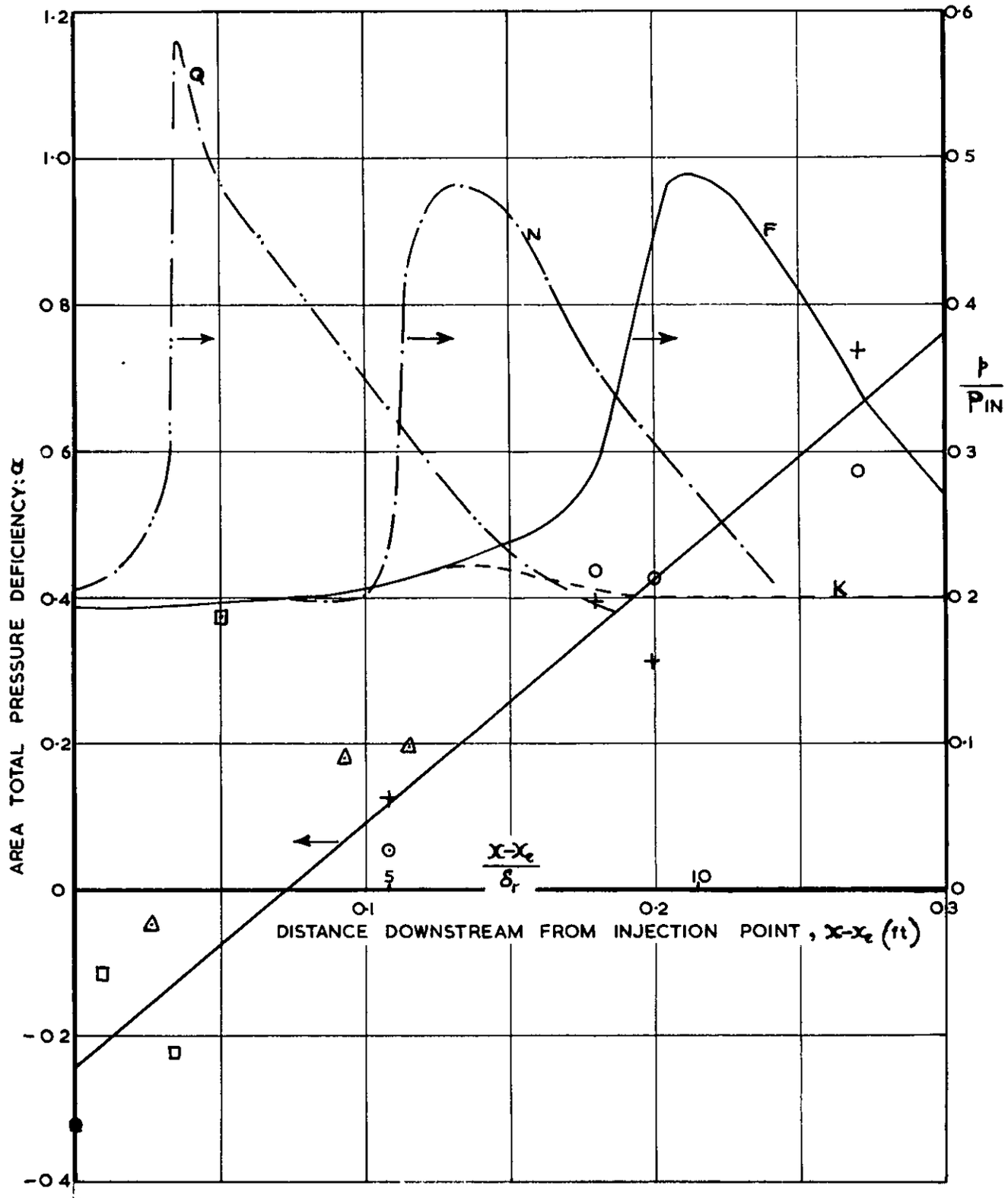

$$\alpha = \frac{\int_0^{\delta} (P_1 - P)\,dy}{\int_0^{\delta_0} (P_1 - P)\,dy_0}$$

KEY

INJECTION AT

$x = 9''$ { ——— F : + ; - - - - - K : ○

$x = 10''$ —— —— —— N : △

$x = 11''$ —— —— ·—— Q . □

$\frac{P_I}{P_{IN}} \sim 2$

AREA TOTAL PRESSURE DEFICIENCY

Printed and published by
HER MAJESTY'S STATIONERY OFFICE
To be purchased from
49 High Holborn, London W C 1
423 Oxford Street, London W 1
13A Castle Street, Edinburgh 2
109 St Mary Street, Cardiff
Brazennose Street, Manchester 2
50 Fairfax Street, Bristol 1
35 Smallbrook, Ringway, Birmingham 5
80 Chichester Street, Belfast 1
or through any bookseller

Printed in England

S.O Code No 23-9016-90